

CATCH & RELEASE THIOL REACTIVE HYDROGELS

by

Merve Coşar

B.S., Chemistry, Boğaziçi University, 2011

Submitted to the Institute for Graduate Studies in
Science and Engineering in partial fulfillment of
the requirements for the degree of
Master of Science

Graduate Program in Chemistry

Boğaziçi University

2012

To my dear family

ACKNOWLEDGEMENTS

First of all, I would like to express my most sincere gratitude to my thesis supervisor Assoc. Prof. Amitav Sanyal for his endless attention and scientific guidance throughout this study. I appreciate his support and useful comments throughout my laboratory work.

I would like to thank Assoc. Prof. Rana Sanyal for her constructive review and comments on the final manuscript.

I would like to thank Assoc. Prof. Sinan Şen for his attending my master thesis defense jury.

I would like to extend my thanks to Bilge Uluocak for her providing the SEM results.

I wish to express my thanks to Tuğçe Nihal GEVREK for her help and support. I also thank Duygu AYDIN for her effort in the synthesis of the pyridyl disulfide monomer. I would like to thank my all labmates for their enjoyable friendship and I would like to thank all my friends and all the members of the faculty in the Chemistry Department.

Finally, my deepest gratitude go to my family for their greatest love, encouragement and support.

This research has been supported by The Scientific and Technological Research Council of Turkey (TUBITAK) (110T068).

ABSTRACT

CATCH & RELEASE THIOL REACTIVE HYDROGELS

Hydrogels have attracted remarkable attention since they have high potential uses in many fields. They are commonly used in tissue engineering, drug delivery systems, biosensors and wound healing dressings. Recently, there is a great interest in fabricating well defined functionalizable hydrogels and hydrogel micropatterns. This study has three parts. In the first part, PEG-based, reversible-thiol reactive hydrogels containing various amount of pyridyl disulfide functional group were synthesized by photopolymerization in the presence of photoinitiator and PEGDMA crosslinker. Swelling studies were conducted and surface morphology of the hydrogels were examined by scanning electron microscopy (SEM). Time-dependent pyridothione release profiles of the bulk hydrogels provided with using glutathione (GSH) were obtained using via UV-vis spectroscopy. As expected, it was found that release of pyridothione depends on thiol-disulfide exchange reaction mechanism. In the second part of the study, PEG-based 3D, reversible-thiol reactive hydrogel micropatterns were fabricated by photopolymerization. Immobilization of thiol containing fluorescent dye, BODIPYC10SH onto the hydrogel micropattern were performed and release of the immobilized molecules from the surface were achieved using GSH and dithiothreitol (DTT). Thiol containing biotin derivatives were covalently attached to the thiol reactive hydrogel micropatterns under mild condition. Immobilization of TRITC-extravidin onto biotinylated hydrogel micropatterns and release of immobilized molecules from the surface were performed using DTT and investigated using fluorescence microscope. In the third part, thiol-reactive orthogonally functionalizable bulk hydrogels containing pyridyl disulfide functional group in certain ratio and additionally various amount of furan protected maleimide functional group were synthesized by photopolymerization. Thermogravimetric analysis of these hydrogels were conducted to demonstrate control over monomer incorporation.

ÖZET

TERSİNİR-TİOL BAĞLANABİLEN HİDROJELLER

Hidrojeller bir çok alanda yüksek kullanım potansiyeline sahip olduklarından oldukça ilgi çeken yapılardır. Hidrojeller, doku mühendisliğinde, ilaç salınım sistemlerinde, biyosensörlerde ve yara iyileştiren giysilerde yaygın olarak kullanılmaktadır. Son zamanlarda iyi yapılanmış ve yapımı kolay hidrojellere ve hidrojel desenlere karşı bir ilgi vardır. Bu çalışma üç bölümden oluşmaktadır. Birinci bölümde, PEG bazlı, tiol gruplarına tersinir biçimde reaktif olan, çeşitli miktarlarda pridil disülfid grubu içeren dökme hidrojeller, fotopolimerizasyon başlatıcı ve PEGDMA çapraz bağlayıcı varlığında fotopolimerizasyon ile sentezlenmiştir. Hidrojellerin su çekme kapasitelerini ölçülmüş ve yüzey morfolijileri elektron taramalı mikroskop (SEM) ile incelenmiştir. Tiol-disülfid değişim reaksiyonu mekanizması kullanılarak, glutatyon (GSH) ile, hidrojellerin zamana bağlı piridotayon salınım profili, ultraviyole-görünür bölge spektroskopisi ile elde edilmiştir. İkinci bölümde, PEG bazlı, üç boyutlu, tiol gruplarına karşı tersinir olarak reaktif olan hidrojel mikrodesenler fotopolimerizasyon ile sentezlenmiştir. Tiol içeren florasan boya moleküllerinin hidrojel desenlere sabitlenmesi ve bağlanan moleküllerin yüzeyden GSH ve DTT ile ayrılması sağlanmıştır. Tiol içeren biyotin türevi, tiol reaktif hidrojel mikrodesenlere oda koşullarında kovalent olarak bağlanmıştır. Biyotinlenmiş hidrojel mikrodesenlere TRITC-extravidin sabitlenmesi ve sabitlenen moleküllerin yüzeyden DTT ile ayrılması sağlanmış ve floresan mikroskobu ile takip edilmiştir. Üçüncü kısımda, belli oranda pridil disülfid ve çeşitli miktarlarda furan korumalı maleimid içeren, tiol gruplarına reaktif ortogonal dökme hidrojeller fotopolimerizasyon ile sentezlenmiştir. Hidrojellerin termogravimetrik analiz çalışmaları, monomer içeriğinin kontrolü için yürütülmüştür.

TABLE OF CONTENTS

ACKNOWLEDGEMENTS	iv
ABSTRACT	v
LIST OF FIGURES	ix
LIST OF TABLES	xi
LIST OF ACRONYMS/ABBREVIATIONS	xii
1. INTRODUCTION.....	1
1.1. Synthesis and Applications of Hydrogels	1
1.2. Functionalizable Hydrogels	2
1.3. Thiol-Disulfide Exchange Chemistry in Polymers and Hydrogels.....	3
1.4. Functionalizable Patterned Hydrogels	7
2. AIM OF THE STUDY	9
2.1. Reversible-Thiol Reactive Bulk Hydrogels	9
2.2. Reversible-Thiol Reactive Hydrogel Micropatterns	9
2.3. Orthogonal Thiol Reactive Bulk Hydrogels	10
3. EXPERIMENTAL	11
3.1. Materials	11
3.2. Measurements and Characterization	11
3.3. Reversible-Thiol Reactive Bulk Hydrogels	12
3.3.1. Synthesis of Bulk Hydrogels	12
3.3.2. Swelling Studies	12
3.3.3. Scanning Electron Microscopy	13
3.3.4. Pyridothione Release Studies	13
3.4. Reversible-Thiol Reactive Hydrogel Micropatterns	14
3.4.1. Modification of Glass Wafer with TMSPMA	14
3.4.2. Fabrication of Hydrogel Micropatterns	14
3.4.3. Immobilization and Release of BODIPYC10SH	14

3.4.4. Immobilization and Release of TRITC-Extravidin	15
3.5. Orthogonal Thiol Reactive Bulk Hydrogels	15
3.5.1. Synthesis of Bulk Hydrogels	15
4. RESULTS AND DISCUSSION	16
4.1. Reversible-Thiol Reactive Bulk Hydrogel.....	16
4.1.1. Synthesis of Bulk Hydrogels	16
4.1.2. Swelling Studies of Bulk Hydrogels.....	18
4.1.3. Surface Morphology Analysis of Bulk Hydrogels	20
4.1.4. Pridothione Release Studies of Bulk Hydrogels.....	21
4.2. Reversible-Thiol Reactive Hydrogel Micropatterns.....	26
4.2.1. Fabrication of Hydrogel Micropatterns	26
4.2.2. Immobilization and Release of BODIPYC10SH	27
4.2.3. Immobilization and Release of TRITC-Extravidin	32
4.3. Orthogonal Thiol Reactive Bulk Hydrogels	35
4.3.1. Synthesis of Bulk Hydrogels	35
4.3.2. Thermogravimetric Analysis of Bulk Hydrogels.....	37
5. CONCLUSION	38
APPENDIX: SPECTROSCOPY DATA	39
REFERENCES	41

LIST OF FIGURES

Figure 1.1. Thiol reactive hydrogels via DA/rDA reaction [23].	3
Figure 1.2. Orthogonal and reversible functionalities in copolymers [24].	4
Figure 1.3. Synthesis of HA-ss-PEG hydrogel [25].	4
Figure 1.4. Formation of nanoaggregates and encapsulation of guest molecules [26].	5
Figure 1.5. Formation of hydrogels with DSDMA and DEDMA crosslinker [27].	6
Figure 1.6. Degradation of DSDMA hydrogel and stability of DEDMA hydrogel [27].	6
Figure 1.7. PDMS microcontact printing to form hydrogel patterns [31].	7
Figure 1.8. Bioimmobilization on a) macroporous and b) non-porous patterns [33].	8
Figure 1.9. Biomolecule penetration in a) macroporous and b) non-porous patterns [33].	8
Figure 2.1. General scheme of the immobilization and release of biomolecules.	9
Figure 4.1. Synthesis of reversible-thiol reactive hydrogels.	16
Figure 4.2. Swelling ratios of hydrogels.	18
Figure 4.3. Effect of pyridyl disulfide content on water uptake.	19
Figure 4.4. Effect of PEG chain length on water uptake.	19
Figure 4.5. SEM images of a) H1 b) H2 c) H3 d) H4 e) H5 f) H6 g) H7 h) H8 i) H9.	20
Figure 4.6. Release of pyridothione molecule from the hydrogel by GSH.	22
Figure 4.7. Pyridothione release profile of H9 at 343 nm.	22
Figure 4.8. Pyridothione release profile of hydrogel H4,H5 and H6.	24
Figure 4.9. Effect of pyridyl disulfide content on pyridothione release.	24
Figure 4.10. Pyridothione release profile of hydrogel H7, H8 and H9.	25
Figure 4.11. Effect of pyridyl disulfide content on pyridothione release.	25
Figure 4.12. Pyridothione release efficiency in H4 and H7, H5 and H8, H6 and H9.	26
Figure 4.13. Preparation of hydrogel micropatterns.	27

Figure 4.14. Optical microscope images of the hydrogel pattern.	27
Figure 4.15. a) Functionalization with BODIPYC10SH. b) Control experiment.	28
Figure 4.16. a) Release of BODIPYC10SH via GSH. b) Control experiment.	29
Figure 4.17. Release of BODIPYC10SH via DTT.	30
Figure 4.18. Fluorescence intensities before and after GSH treatment, and control.	31
Figure 4.19. Fluorescence intensities before and after DTT treatment, and control.	31
Figure 4.20. Immobilization and release of TRITC-extravidin.	33
Figure 4.21 a) Control experiment. b) Functionalization with TRITC-extravidin.	33
Figure 4.22. Release of TRITC-extravidin via DTT.	34
Figure 4.23. Fluorescence intensities before and after DTT treatment and control.	34
Figure 4.24. Synthesis of orthogonal thiol reactive bulk hydrogels.	36
Figure 4.25. Thermogravimetric analysis of the hydrogels.	37
Figure A.1. Thermogravimetric analysis of the H1.	39
Figure A.2. Thermogravimetric analysis of the H2.	39
Figure A.3. Thermogravimetric analysis of the H3.	40

LIST OF TABLES

Table 4.1. Properties of bulk hydrogels.	17
Table 4.2. Maximum pyridothione release efficiency (%) of the hydrogels.	23
Table 4.3. Properties of bulk hydrogels.	36

LIST OF ACRONYMS/ABBREVIATIONS

DA	Diels-Alder
DCM	Dichloromethane
DMPA	2, 2-Dimethoxy-2-phenylacetophenone
DMSO	Dimethylsulfoxide
DEGMEMA	Diethylene Glycol Methacrylate
DTT	Dithiothreitol
FuMaMA	Furan Protected Maleimide Methacrylate
GSH	Glutathione
M _w	Molecular Weight
PBS	Phosphate Buffered Saline
PDMS	Polydimethylsiloxane
PDSMA	Pyridyl Disulfide Methacrylate
PEGMEMA	Polyethylene Glycol Methyl Ether Methacrylate
PEGDMA	Polyethylene Glycol Dimethacrylate
PEG	Polyethylene Glycol
rDA	Retro Diels-Alder reaction
SEM	Scanning Electron Microscopy
TGA	Thermogravimetric Analysis
TMSPMA	3-Trimethoxysilyl Propyl Methacrylate
THF	Tetrahydrofuran

1. INTRODUCTION

1.1. Synthesis and Applications of Hydrogels

In recent years, fabrication of biocompatible hydrogels, biological polymers, and three-dimensional (3D) biomaterials have drawn significant attention in biomedical sciences [1]. Hydrogels are crosslinked polymeric structures that are capable of uptaking water and they can be synthesized via physical interactions or chemical crosslinking. When the networks are constructed by molecular entanglements or secondary forces such as ionic interaction, H-bonding or hydrophobic forces they are called physical gels [2-3].

However, physical interactions cannot always yield stable and robust gels [4]. In order to obtain stable, non-reversible and robust hydrogels, chemical crosslinking is applied. Examples for chemically crosslinked hydrogel networks with the most commonly used mechanisms can be given as; azide functionalized PVA's clicked with alkyne appended PVA's [5], polymerization of peptides with ATRP [6], crosslinking with Diels-Alder reaction between PEG-bismaleimide and furan containing polymers [7], PEG-tetrathiols clicked with bisacrylates [8] to give hydrogel networks and photo crosslinking of acrylates in the presence of a photoinitiator [9].

The high water content makes hydrogels biocompatible and owing to their resemblance to natural tissues, hydrogels have become very popular materials and they have been used and tried in many application areas in a few decades. They can be applied for biomolecular immobilization, tissue engineering, drug delivery, biosensors, contact lenses and wound healing dresses [10-13]. Hydrogels can be used as scaffolds for cell growth in tissue engineering. They can be used as drug carriers and drug release can be monitored. They can become responsive to biomolecules and used as biosensors. Hydrogels are applicable for wound healing since they can provide moisture to the wound, relieve the pain and facilitate to healing [14]. It can be said that hydrogel have high potential of use for many different fields and they can be applied to new areas by creating novel structures.

1.2. Functionalizable Hydrogels

Functionalization of hydrogels can be performed by covalent or non-covalent attachment of biomolecules. Covalent attachment methods are preferred for applications such as bioimmobilization, controlled drug delivery and tissue engineering in order to obtain controlled attachment.

Since hydrogels can encapsulate various guest molecules, they can be used as scaffolds. These guest molecules can be peptides or drug molecules that can be slowly released into the vicinity of an implant [15] or growth factors or signaling peptide molecules for cell culture and tissue engineering applications [16]. The functionalization of the hydrogels with desired molecules can be achieved by physisorption and by covalent attachments methods. However, since physisorption has limitations due to the lack of control over rate and uniformity, hydrogels containing covalently attached biomolecules are widely applied. Generally, a monomer of the desired biomolecule is synthesized in order to immobilize biomolecules on hydrogels. For example, a photo-crosslinked hydrogel scaffold containing covalently immobilized gradients of basic fibroblast growth factor (bFGF) by using PEG-diacrylate and acryloyl-PEG-RGDS were fabricated by West and coworkers. It was observed that within 24 hours, cells seeded on this hydrogel were aligned in the direction of increasing bFGF concentration [17]. As a later study, they synthesized hydrogels containing covalently attached biotin and the cell adhesive peptide RGDS. They utilized a PEG monomer containing an activated ester at one terminus and the acrylate group at the other end. The activated ester group provides attachment of any molecule of interest through the amidation chemistry and the acrylate group allows covalent integration into the hydrogel and creates 3D patterns via single photon absorbance (SPA) photolithography [18].

An alternative and more convenient strategy is to immobilize biomolecules on hydrogels through post-functionalization [19]. In this approach, hydrogels have reactive functional groups and provide efficient immobilization under mild reaction conditions. For immobilization of biomolecules, a much sought after functionalization is via thiols since many biomolecules either contain or can be incorporated with cysteine residues at specific

sites. Sulfhydryl group of the cysteine residues in biomolecules undergo facile reactions with maleimides [20], ortho pyridyl disulfide units [21], and vinyl sulfones [22].

In 2010, Sanyal *et al.* showed the fabrication of thiol reactive hydrogels containing maleimide functional groups [23]. In this work, novel hydrogels were synthesized with using furan protected maleimide methacrylate with PEGMA. By retro Diels-Alder reaction, some furan molecules were removed and *in situ* crosslinking polymerization occurs. After that, remaining free maleimides were activated and thiol containing dye and enzyme were immobilized on thiol reactive hydrogels (Figure 1.1).

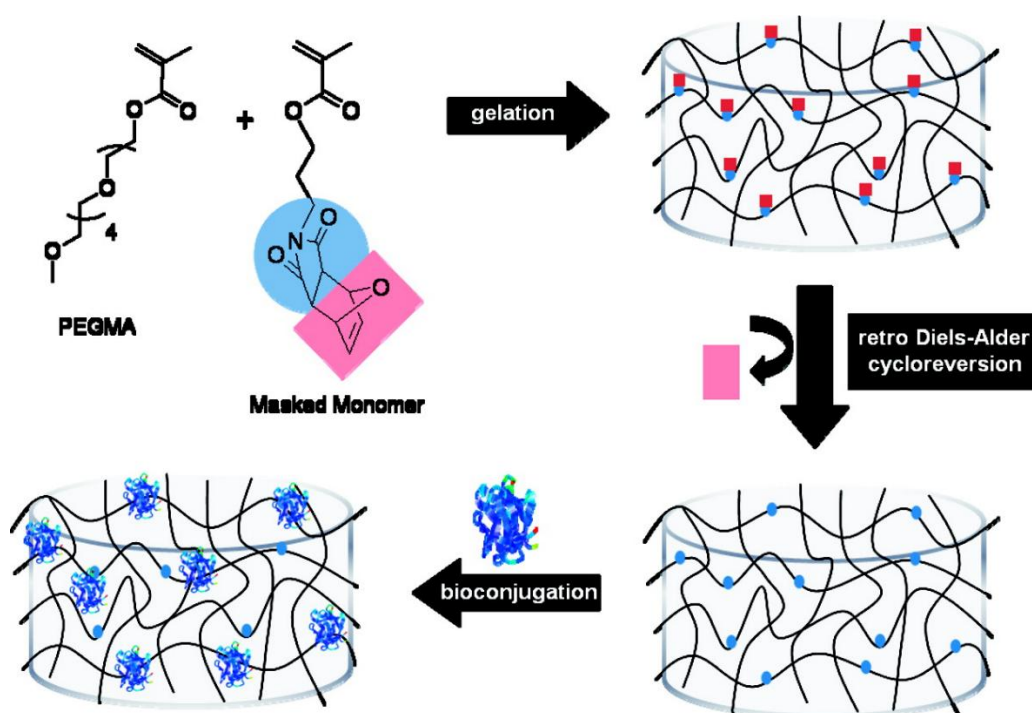


Figure 1.1. Thiol reactive hydrogels via DA/rDA reaction [23].

1.3. Thiol-Disulfide Exchange Chemistry in Polymers and Hydrogels

In 2006, Thayumanavan *et al.* presented a new methodology to form multiple functional groups containing polymers [24]. In this study, they performed copolymerization of *N*-hydroxysuccinimide methacrylate and pyridyl disulfide

methacrylate by ATRP, and synthesized copolymer has two functional groups that are reactive towards thiols and amines. Disulfide linkages on the backbone of the copolymer provide reversible attachment of a molecule (Figure 1.2)

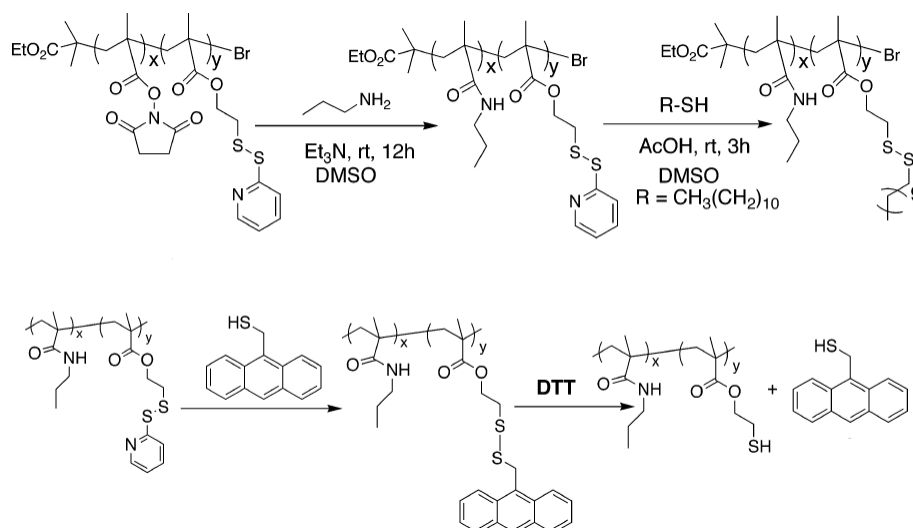


Figure 1.2. Orthogonal and reversible functionalities in copolymers [24].

In 2011, Wang *et al.* showed the synthesis of injectable hyaluronic acid hydrogels using HA derived pyridyl disulfide and PEG-dithiol acting as a crosslinker via thiol disulfide exchange reaction as shown in Figure 1.3. The process tuned by release of pyridothione molecule that provides quantitative hydrogel formation by UV spectroscopy. In the study, it was shown that produced hydrogels are degradable in the presence of hyaluronidase enzyme and since the hydrogels have disulfide bonds, they were found to be also degradable in the presence of thiol containing reagent like glutathione. They indicated that HA-ss-PEG hydrogels can be useful for protein encapsulation and delivery, also can be applicable for several types of cell encapsulation [25].

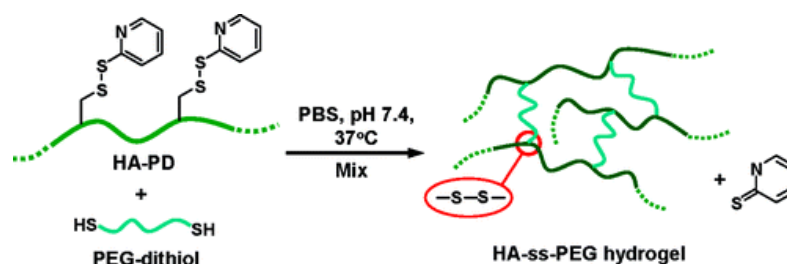


Figure 1.3. Synthesis of HA-ss-PEG hydrogel [25].

In 2010, Thayumanavan *et al.* showed the preparation of biocompatible nanogels formed by random copolymer containing oligoethyleneglycol (OEG) and pyridyldisulfide (PDS) units via intra-/intermolecular disulfide cross-linking process depending on thiol-disulfide exchange mechanism. In the study, in order to create thiol groups in the copolymer, deficient amount of DTT was used and produced thiol groups react with the remaining pyridyl disulfide units and provide the formation of nanogels. They showed that the nanoaggregates are appropriate for encapsulation of hydrophobic dye and drug molecules (Figure 1.4). Since nanogels have disulfide bonds that are cleavable in the presence of reducing agent, they were found to be degradable in the presence of glutathione. By using this property, the release of noncovalently encapsulated hydrophobic molecules were achieved with using thiol containing reagent, glutathione and release kinetics can be monitored by changing the crosslinking density of the nanogels [26].

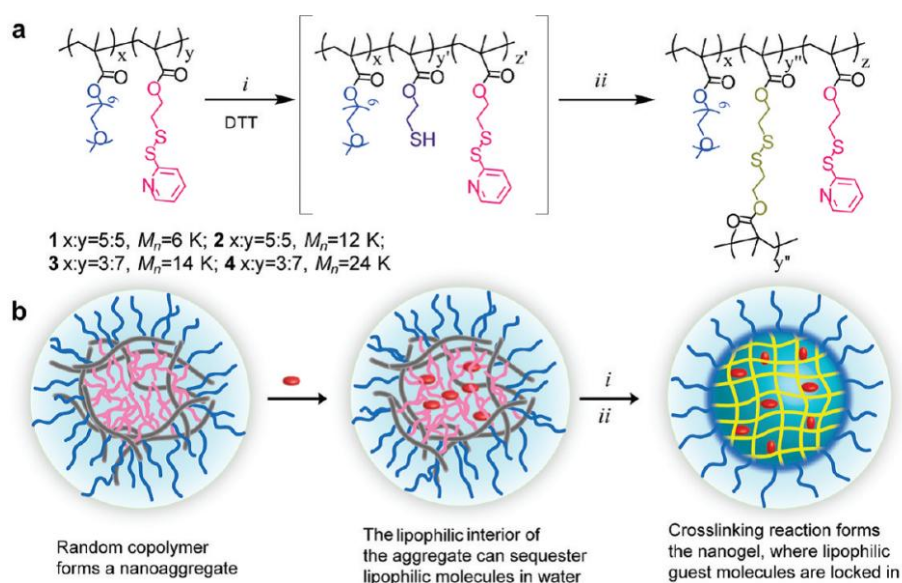


Figure 1.4. Formation of nanoaggregates and encapsulation of guest molecules [26].

In 2011, Grayson *et al.* synthesized PHEMA based hydrogel with different crosslinkers; DSDMA and DEDMA that have disulfides and ether linkages respectively as shown in Figure 1.5. They showed that the hydrogel formed with disulfide linkage containing crosslinker was degradable in the presence of glutathione by thiol-disulfide exchange reaction and the release of loaded molecules can be achieved (Figure 1.6) [27].

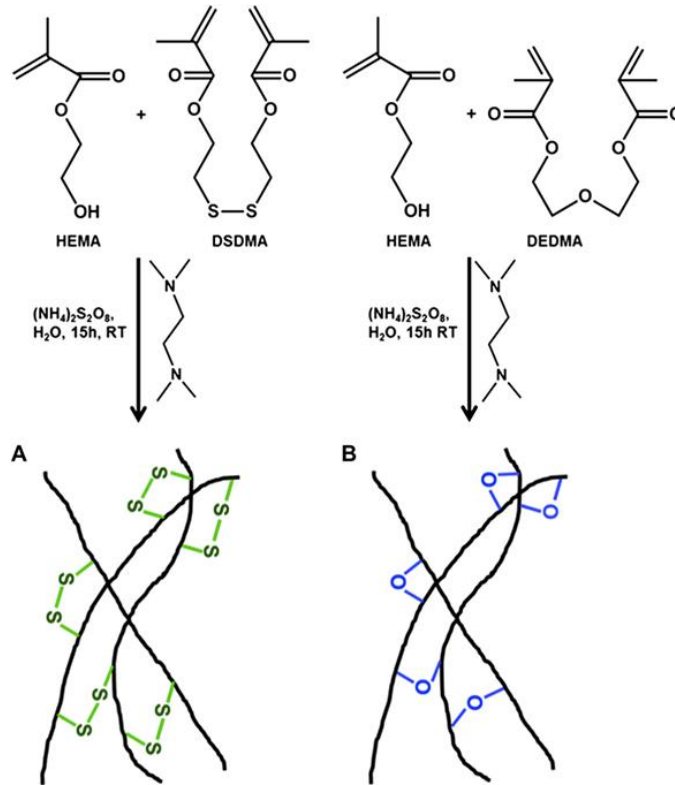


Figure 1.5. Formation of hydrogels with DSDMA and DEDMA crosslinker [27].

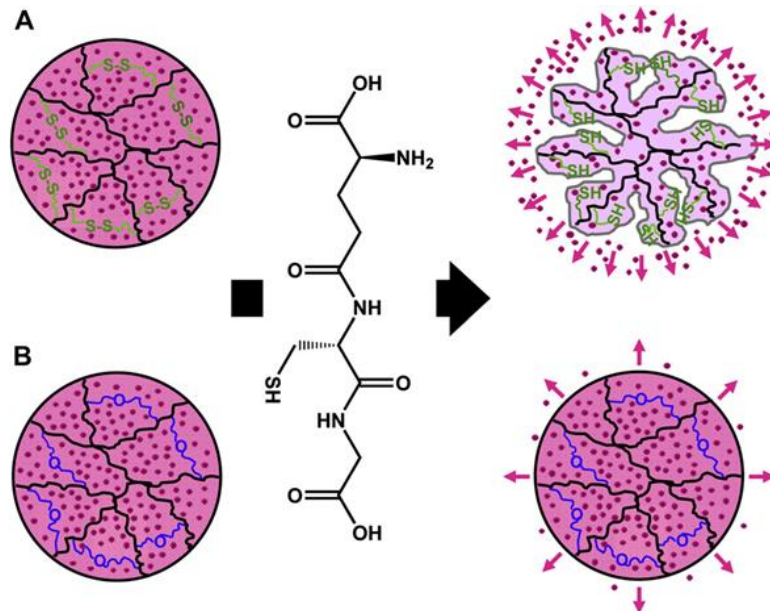


Figure 1.6. Degradation of DSDMA hydrogel and stability of DEDMA hydrogel [27].

1.4. Functionalizable Patterned Hydrogels

There are many ways to fabricate hydrogel patterns like photoreaction injection [28], photolithography [29], microfluidic patterning [30], microcontact printing [31] and electrochemical deposition [32]. As an example for microcontact printing method, Chirra *et al.* fabricated hydrogel patterns by using PDMS stamping via atom transfer radical polymerization (ATRP) as shown in Figure 1.7 [31].

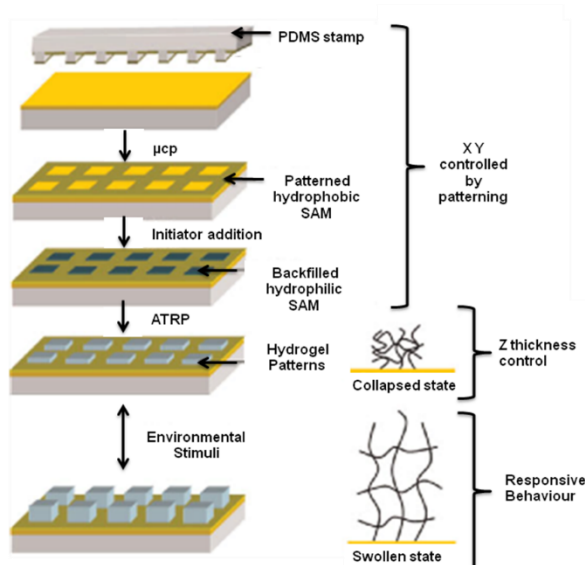


Figure 1.7. PDMS microcontact printing to form hydrogel patterns [31].

Also photopolymerization method is widely used to produce hydrogel patterns for biomolecule immobilization and patterns that are suitable to immobilize protein are widely applied mostly in biosensors, bioMEMS, tissue engineering. Koh *et al.* introduced an effective way to obtain poly(2-hydroxyethyl methacrylate) (PHEMA) based macroporous hydrogel micropatterns for protein immobilization via photopolymerization [33]. In the study, in order to get macroporous hydrogel structure, polystyrene nanoparticles were used. They showed that the immobilization of different biomolecules on hydrogel micropatterns and compared the efficiency of immobilization on between macroporous and non-porous patterns. It was found that the macroporous patterns show higher efficiency to immobilize biomolecules as shown in Figure 1.8 and allow biomolecules to diffuse in the inner layers

of the hydrogel patterns fully comparing to the situation in terms of non-porous patterns as shown in Figure 1.9.

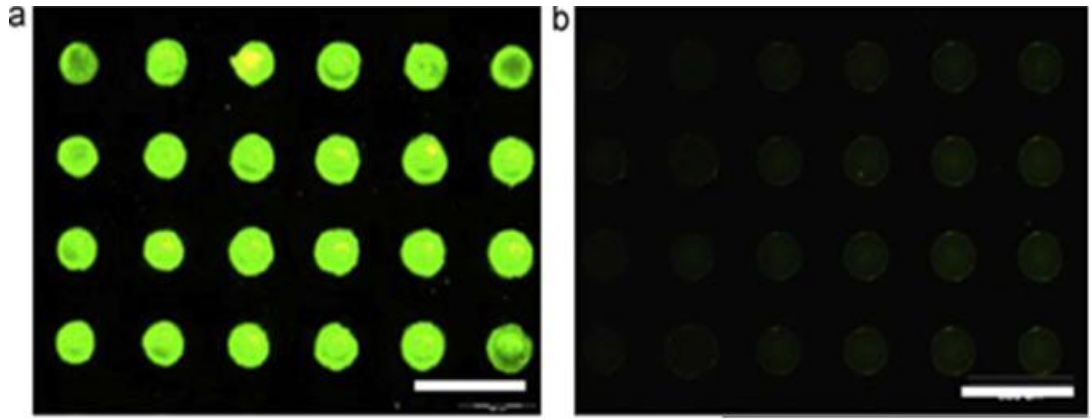


Figure 1.8. Bioimmobilization on (a) macroporous and (b) non-porous patterns [33].

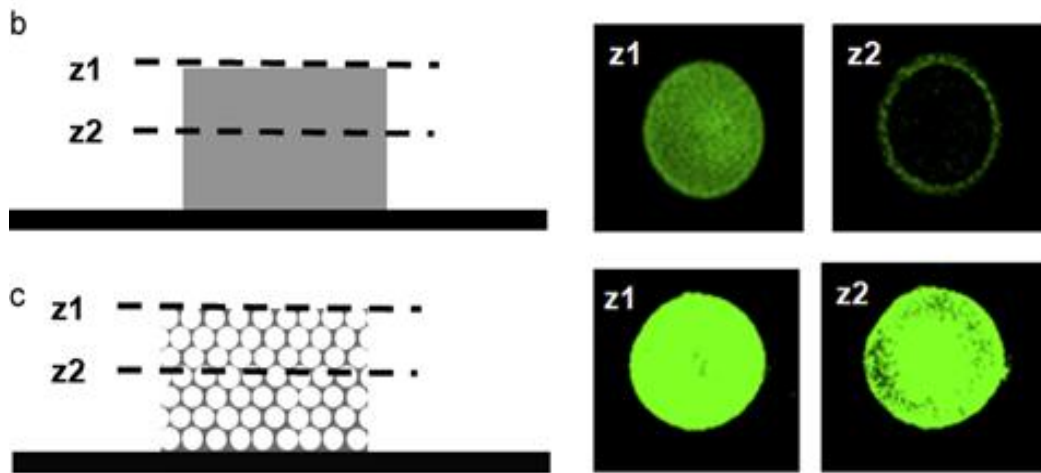


Figure 1.9. Biomolecule penetration in a) macroporous and b) non-porous patterns [33].

There are many biomedical applications of photopolymerized hydrogels like prevention of thrombosis [34], post-operative adhesion formation [35], drug delivery [36], coatings for biosensors [37], and for cell transplantation [38].

2. AIM OF THE STUDY

2.1. Reversible-Thiol Reactive Bulk Hydrogels

In the first part of the study, the aim is to produce novel, reversible-thiol reactive bulk hydrogels containing pyridyl disulfide units that can be react with the thiol containing molecules via thiol-disulfide exchange mechanism. By using thiol containing reducing agent GSH, release profile of the pyridothione molecule of the bulk hydrogels will be investigated. Amount of release, swelling property and surface morphology of the hydrogels can be tuned by using various amount of pyridyl disulfide containing monomer and by using PEG polymers with different chain lengths.

2.2. Reversible-Thiol Reactive Hydrogel Micropatterns

In the second part of the study, fabrication of hydrogel micropatterns containing pyridyl disulfide functional groups will be undertaken. These micropatterns will be functionalized with thiol containing fluorescent dye to study the catch and release of a thiol bearing molecule. Release of the dye molecules by using different thiol containing reducing agents will be studied. Also catch and release of the protein onto biotinylated hydrogel micropatterns will be demonstrated (Figure 2.1).

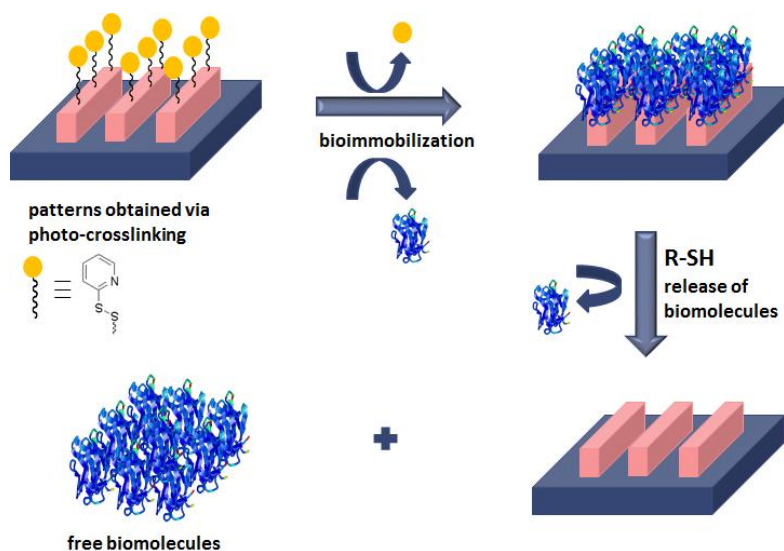


Figure 2.1. General scheme of the immobilization and release of biomolecules.

2.3. Orthogonal Thiol Reactive Bulk Hydrogels

In the third part of the study, the aim is to prepare both pyridyl disulfide and various amount furan of protected maleimide functional group containing bulk hydrogels. Thermogravimetric analysis studies will be shown.

3. EXPERIMENTAL

3.1. Materials

The pyridyl disulfide methacrylate (PDSMA) monomer [24] and the furan protected maleimide methacrylate (FuMaMA) monomer were synthesized according to literature procedure [39]. Diethylene glycol methyl ether methacrylate (DEGMEMA, $M_w = 188$), Polyethylene glycol methyl ether methacrylate (PEGMEMA, $M_w = 300$ and $M_w = 1100$), Polyethylene glycol dimethacrylate (PEGDMA, $M_w = 550$) were purchased from Sigma Aldrich and purified before using by passing through the aluminum oxide column. Methacryloyl chloride was obtained from Alfa Aesar. Triethylamine (TEA), 2,2-Dimethoxy-2-phenylacetophenone (DMPA), 3-trimethoxysilyl propyl methacrylate (TMSPMA), L-glutathione (GSH) and TRITC-extravidin were purchased from Sigma Aldrich. L-dithiothreitol (DTT) was obtained from Fluka. Biotinylated (triethylene glycol) undecanethiol (Biotin-SH) was obtained from Nanoscience Instruments (Phoenix, AZ). 4,4-Difluoro-1,3,5,7-tetramethyl-8-[(10-mercapto)]-4-bora-3a,4a-diaza-s-indacene (BODIPYC10SH) was synthesized according to literature procedure [40]. Other chemical reagents were obtained from commercial resources and were used as received. Anhydrous solvents such as dichloromethane (DCM), tetrahydrofuran (THF) and toluene were obtained from SciMatCo purification system and other solvents were dried over molecular sieves. Column chromatography was performed using silica gel 60 (43-60 nm, Merck). Thin layer chromatography was performed using silica gel plates (Kieselgel 60 F254, 0.2 mm, Merck). The plates were viewed under 254 nm UV lamp otherwise plates were developed either by $KMnO_4$ stain.

3.2. Measurements and Characterization

In order to remove water from hydrogels LabConco lyophilizer was applied. In order to characterize the surface morphology of the bulk hydrogels, electron microscopy (SEM) observation was performed with ESEM-FEG/EDAX Philips XL-30 (Philips, Eindhoven, The Netherlands) operating at 10 kV. Hydrogel precursors were

photopolymerized through Blak-Ray, B-100 AP/R High Intensity UV Lamp (100W, 365 nm). Thermogravimetric analysis (TGA) was carried out with a TGA Q50 from TA instruments at a heating sample from ambient temperature to 600 °C at a rate of 10 °C/min under a nitrogen flow (100 mL/min) demonstrate control over monomer incorporation by observing weight loss (%) due to furan release from the hydrogels. UV-vis spectra of pyridothione release data were collected by Cary Varian UV-vis spectrophotometer. Fluorescence microscopy (HBO100 ZEISS Fluorescence Microscopy, Carl Zeiss Canada Ltd, Canada) was applied in order to confirm the immobilization of BODIPYC10SH and TRITC-extravidin onto hydrogel pattern and release of immobilized BODIPYC10SH and TRITC-extravidin from the hydrogel pattern.

3.3. Reversible-Thiol Reactive Bulk Hydrogels

3.3.1. Synthesis of Bulk Hydrogels

Bulk hydrogels were synthesized by UV initiated free radical photopolymerization at ambient temperature. Three series of bulk hydrogels containing various amount of pyridyl disulfide monomer were prepared and each group has different hydrophilic monomer that are DEGMEMA ($M_w = 188$), PEGMEMA ($M_w = 300$) and PEGMEMA ($M_w = 1100$) (Table1). For the first group, various amount of PDSMA, and PEGMEMA as monomers, PEGDMA as a crosslinker, DMPA as a photoinitiator, DMSO as a solvent were mixed in transparent glass vial and sonicated for 5 min at room temperature. The mixture was exposed to UV-light (100W, 365 nm) for 30 min at room temperature and photopolymerization of the bulk hydrogels was conducted. In order to get rid of unreacted reactants, the synthesized bulk hydrogels were washed with THF several times and also they were washed with distilled/deionized water and then dried by lyophilization for 12 hours.

3.3.2. Swelling Studies

A small piece of dry hydrogel was transferred to a flask containing distilled/deionized water at room temperature. At regular intervals, the weight of the

hydrogel sample is recorded after removing the hydrogel from the water and drying the surface moisture with a tissue paper. The water uptake percentage (W_{up}) was calculated by applying the following equation:

$$W_{up}(\%) = (W_{max} - W_{dry}) / W_{dry} \times 100$$

3.3.3. Scanning Electron Microscopy

In order to examine the surface morphology of the hydrogels scanning electron microscopy was used. Dry hydrogel samples were introduced to ESEM-FEG/EDAX Philips XL-30 (Philips, Eindhoven, The Netherlands) instrument using an accelerating voltage of 10 kV and SEM images were taken.

3.3.4. Pyridothione Release Studies

Pyridothione release studies of H1, H2, H3, H4, H5, H6, H7, H8, H9 were conducted. 2 mg of bulk hydrogel sample of each bulk hydrogel were transferred into 3 ml of 10 mM GSH solution with PBS at pH 7.4 in glass vials. Glass vials containing solutions were put in the oil bath and stirred at 37 °C. At regular intervals, solutions were introduced into Cary Varian UV-vis spectrophotometer and UV-vis spectra data giving pyridothione releases from the bulk hydrogels at 343 nm were collected. Pyridothione release percentages of bulk hydrogels upon time were calculated from the formula of $A = \epsilon bc$ where ϵ is the extinction coefficient of the absorber, b is the length of the light path, c is the molar concentration. The values were taken as $\epsilon = 8.08 \times 10^3 \text{ M}^{-1}\text{cm}^{-1}$, $b = 1 \text{ cm}$, also absorbance value was obtained from Cary Varian UV-vis spectrophotometer and molar concentration was calculated. From calculated molar concentration, by applying $M = n(\text{mol})/V(\text{L})$ and taking $V = 3 \times 10^{-3} \text{ L}$, released mol of pyridothione was obtained. Since this value is equal to the mol of PDSMA and theoretical mol of PDSMA in 2 mg of bulk hydrogel sample is known, by applying the formula of ; $n_{\text{released}}(\%) = (n_{\text{actual}} / n_{\text{theoretical}}) \times 100$, pyridothione release percentages of bulk hydrogels were calculated.

3.4. Reversible-Thiol Reactive Hydrogel Micropatterns

3.4.1. Modification of Glass Wafer with TMSPMA

In order to promote the covalent adhesion between the glass surface and the hydrogel, the glass surface was modified with TMSPMA. Glass wafer was soaked in a 10% (by weight) solution of TMSPMA in anhydrous toluene for 12 hours at room temperature. The modified glass surface was washed several times in toluene and methanol and then dried under vacuum.

3.4.2. Fabrication of Hydrogel Micropatterns

The PDMS stamp was carefully placed on the surface of the TMSPMA modified glass wafer. The mixture containing bulk hydrogel precursors of hydrogel H1 and DCM as a solvent instead of DMSO was dropped at one of the open ends of PDMS stamp channels on the glass wafer and the channel of PDMS was filled with the mixture. The glass wafer with PDMS channel filled with the mixture was placed under UV lamp and exposed to UV-light (100W, 365 nm) for 40 min. After photopolymerization process, PDMS stamp was taken off from the glass surface and hydrogel micropatterns on the surface were washed with THF to remove any unreacted reactants.

3.4.3. Immobilization and Release of BODIPYC10SH

The reversible-thiol reactive hydrogel micropattern containing pyridyl disulfide functional groups was incubated in the solution of BODIPYC10SH (1 mg) in THF (1 mL) overnight and the pattern was washed several times with THF in order to get rid of unbound BODIPYC10SH and fluorescent images were taken. As a control, the hydrogel pattern that was fabricated without pyridyl disulfide monomer was incubated in the solution of BODIPYC10SH (1 mg) in THF (1 mL) overnight and the pattern were washed several times with THF to remove unbound fluorescent dye molecules and fluorescent images were taken. The BODIPYC10SH immobilized pattern containing pyridyl disulfide functional groups was incubated in GSH solution (20 mM) overnight and washed several

times with THF and fluorescent images were taken. As a control, BODIPYC10SH immobilized, pyridyl disulfide functional group containing pattern was incubated in THF-water solution overnight and fluorescent images were taken.

3.4.4. Immobilization and Release of TRITC-Extravidin

Reversible-thiol reactive hydrogel patterns were treated with 3 mg BiotinSH in 2 ml MeOH solution and reacted overnight. Biotinylated patterns were washed several times with MeOH and incubated in the solution of TRITC-extravidin (0.2 mg/mL PBS) for 60 minutes. Protein immobilized patterns were washed several times with water and fluorescence microscope images were taken. As a control, a hydrogel pattern that was not biotinylated was incubated in TRITC-extravidin solution and washed several times with water and fluorescence microscope images were taken.

3.5. Orthogonal Thiol Reactive Bulk Hydrogels

3.5.1. Synthesis of Bulk Hydrogels

Bulk hydrogels were synthesized by UV initiated free radical photopolymerization at ambient temperature. A series of bulk hydrogels was synthesized. A certain amount of pyridyl disulfide monomer, various amount of furan protected maleimide monomer and PEGMEMA ($M_w = 300$) as hydrophilic monomer, PEGDMA as a crosslinker, DMPA as a photoinitiator, DMSO as a solvent were mixed in transparent glass vial and sonicated for 5 min at room temperature. The mixture was exposed to UV-light (100W, 365 nm) for 30 min at room temperature and photopolymerization of the bulk hydrogels was conducted. In order to get rid of unreacted reactants, the synthesized bulk hydrogels were washed with THF several times and also they were washed with distilled/deionized water and then dried by lyophilization for 12 hours.

4. RESULTS AND DISCUSSION

4.1. Reversible-Thiol Reactive Bulk Hydrogel

4.1.1. Synthesis of Bulk Hydrogels

PEG-based reversible-thiol reactive bulk hydrogels containing various amount of pyridyl disulfide functional groups were synthesized by photopolymerization in the presence of DMPA as a photoinitiator and PEGDMA as a crosslinker (Figure 4.1). The physical and chemical properties of the hydrogels show differences due to changes in the parameters used like ratio between pyridyl disulfide monomer and hydrophilic monomer or chain length of the hydrophilic monomer. In order to investigate the role of each of these two parameters a variety of hydrogels were synthesized. These results are summarized in Table 4.1. Gelations proceeded with good conversions within 30 minutes for low molecular weight monomers but a remarkable decrease in conversion was observed for the PEG monomer (Mw= 1100) containing a longer PEG unit.

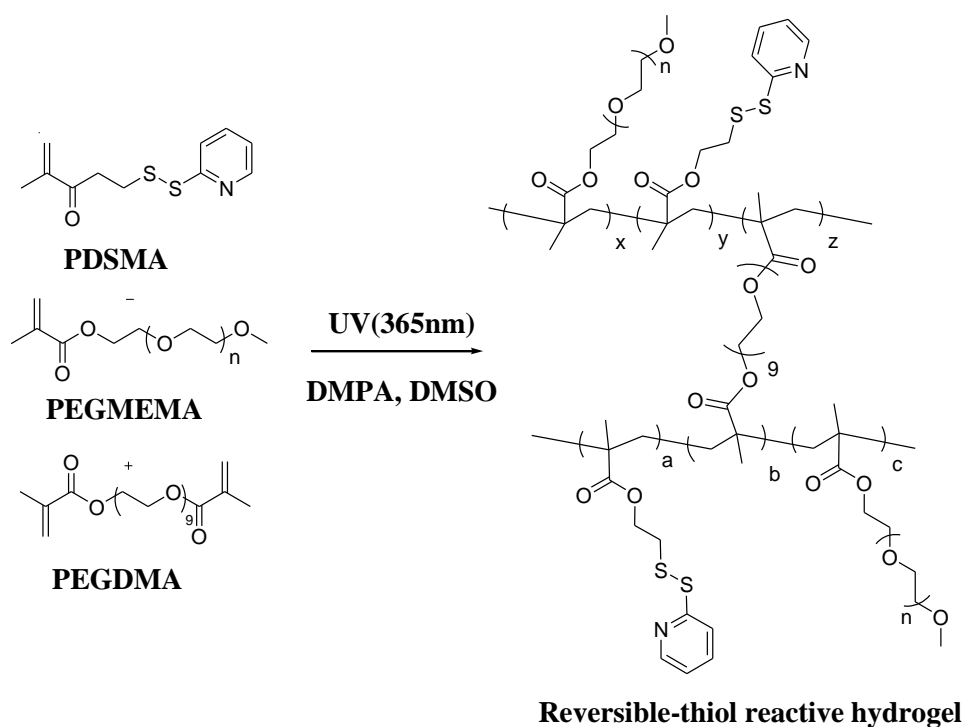


Figure 4.1. Synthesis of reversible-thiol reactive hydrogels.

Table 4.1. Properties of bulk hydrogels.

Hydrogels	Monomer	Monomer M_w	Ratio of PDSM:monomer (%)	Conversion (%)
H1	DEGMEMMA	188	10 : 90	79.5
H2	DEGMEMMA	188	20 : 80	99.5
H3	DEGMEMMA	188	40 : 60	85.5
H4	PEGMEMMA	300	10 : 90	91.8
H5	PEGMEMMA	300	20 : 80	83.9
H6	PEGMEMMA	300	40 : 60	90.0
H7	PEGMEMMA	1100	10 : 90	36.0
H8	PEGMEMMA	1100	20 : 80	33.9
H9	PEGMEMMA	1100	40 : 60	40.5

Photopolymerization condition; PEGDMA = 14.2 mg, DMPA = 5 mg, DMSO = 0.020 mL, UV (365 nm) illumination time = 30 min, room temperature. Conversion (%) = (dry gel weight / total weight of monomer) × 100.

4.1.2. Swelling Studies of Bulk Hydrogels

Swelling studies of the bulk hydrogels were conducted and Figure 4.2 shows the swelling study results for the all of nine different bulk-hydrogels. According to the obtained results, as the PDSMA content increases within the hydrogel, water uptake capacity of the hydrogel decreases due to increasing hydrophobic character of the hydrogels (Figure 4.3). Also it was found that as PEG chain length plays an important role in swelling ratio. Since PEG is hydrophilic polymer, as PEG chain length increases, the hydrogel becomes more hydrophilic and swelling ratio of the hydrogels increases (Figure 4.4).

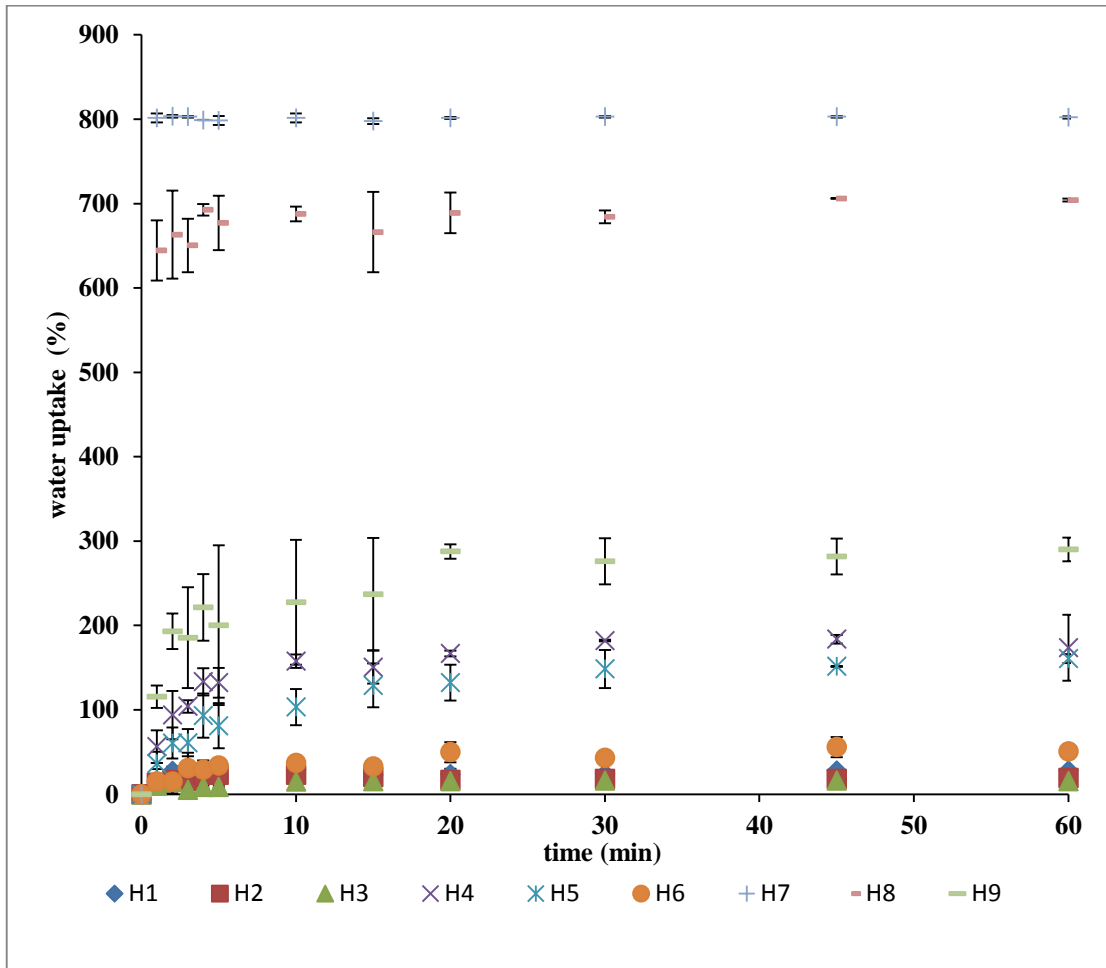


Figure 4.2. Swelling ratios of hydrogels.

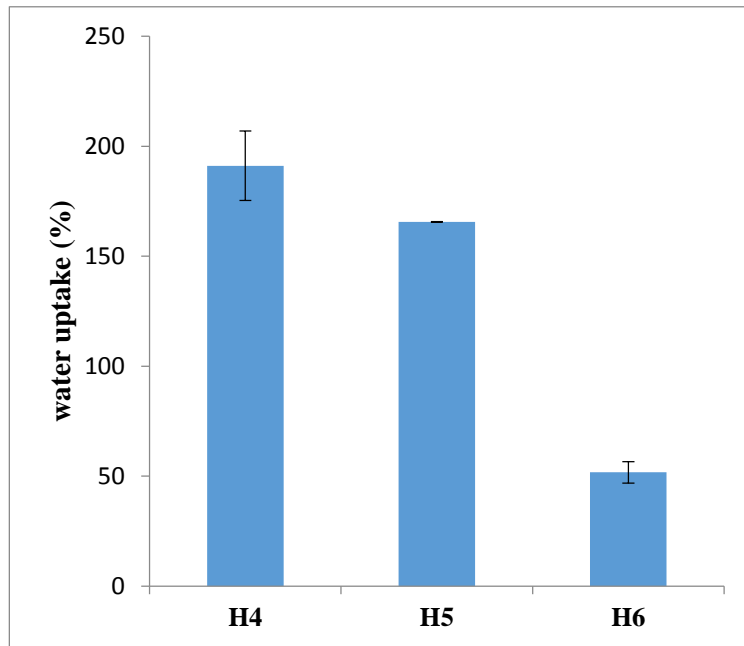


Figure 4.3. Effect of pyridyl disulfide content on water uptake.

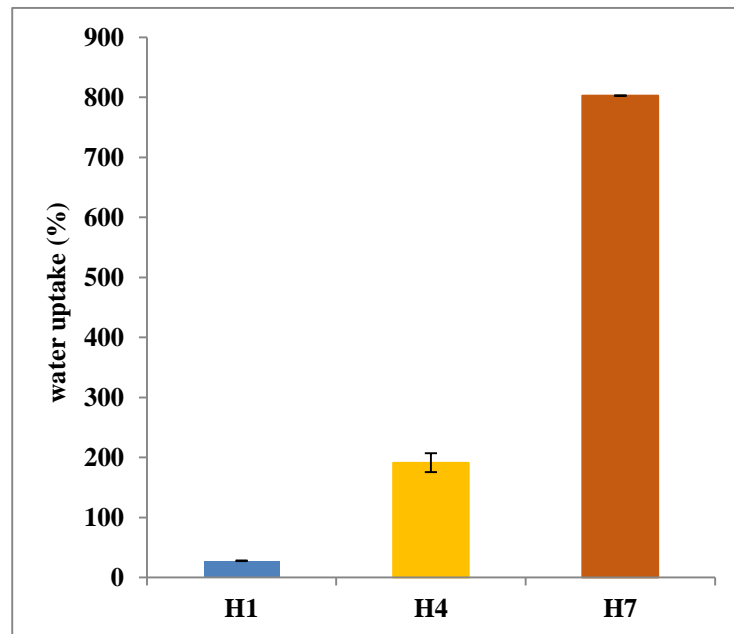


Figure 4.4. Effect of PEG chain length on water uptake.

4.1.3. Surface Morphology Analysis of Bulk Hydrogels

Surface morphology of the hydrogels were examined via scanning electron microscopy. SEM micrographs show that as PDSMA content of the hydrogels increases, less microporous structures were obtained due to increasing hydrophobicity of the hydrogels. As PEG chain length increases, because of increasing hydrophilicity character more microporous structures were obtained (Figure 4.5). For example, hydrogels H1, H2, H3 have non-porous structures as compared to H4, H5 and H6 that were synthesized with higher molecular weight of PEGMEMA. Similarly, H4, H5 and H6 have less porous structures comparing to hydrogels H7, H8 and H9 that were synthesized by using hydrophilic PEGMEMA with longest chain length. Also, it was observed that there is an obvious relationship between microporosity degree and water uptake capacity of the hydrogels. By looking the obtained data about SEM images and swelling graphs, it is inferred that the hydrogels showing more microporous structures have higher swelling degree.

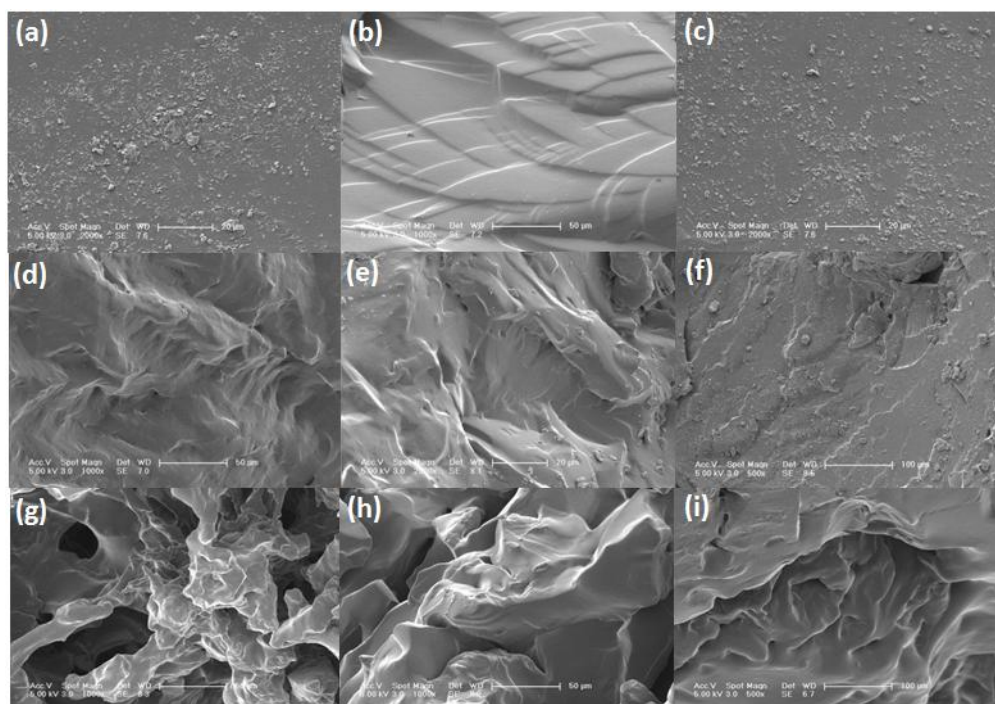


Figure 4.5. SEM images of a) H1 b) H2 c) H3 d) H4 e) H5 f) H6 g) H7 h) H8 i) H9.

4.1.4. Pyridothione Release Studies of Bulk Hydrogels

Since the synthesized hydrogels have pyridyl disulfide functional groups, in the presence of thiol containing reagent, thiol disulfide exchange reaction occurs. When the hydrogels having pyridyl disulfide units are treated with GSH solution, thiol groups of GSH cleaves the disulfide bonds of the hydrogels and as a result pyridothione molecule is released (Figure 4.6). Since this molecule has a specific absorbance value at 343 nm, the pyridothione release profiles of the hydrogels having various amount of pyridyl disulfide units were obtained via UV-vis spectrophotometer instrument. Figure 4.7 shows the pyridothione release of hydrogel H9 up to 6 hours. Table 4.2. indicates the maximum pyridothione release percentage of the hydrogels. According to the results obtained, pyridyl disulfide content affects the release profiles. Increase in pyridyl disulfide units within the hydrogel leads to decrease in pyridothione release percentage. As hydrophobic pyridyl disulfide monomer amount increases, PEG units within the hydrogel decreases and hydrogel gains more hydrophobic character and this situation makes harder pyridothione release. Figure 4.8 and 4.9 show the pyridothione release trend for hydrogels synthesizing with 300 g/mol molecular weight and with various amount of PDSMA. Figure 4.10 and 4.11 show the pyridothione release trend for hydrogels preparing with 1100 g/mol molecular weight and with various amount of PDSMA.

Another significant factor affecting the release amount was found as PEG chain length. Since PEGMEMA has hydrophilic property, increase in chain length yields more hydrophilic hydrogel formation and makes easier pyridothione to release, so hydrogels that were synthesized with higher molecular weight of PEGMEMA leads to higher amount of pyridothione release (Figure 4.12).

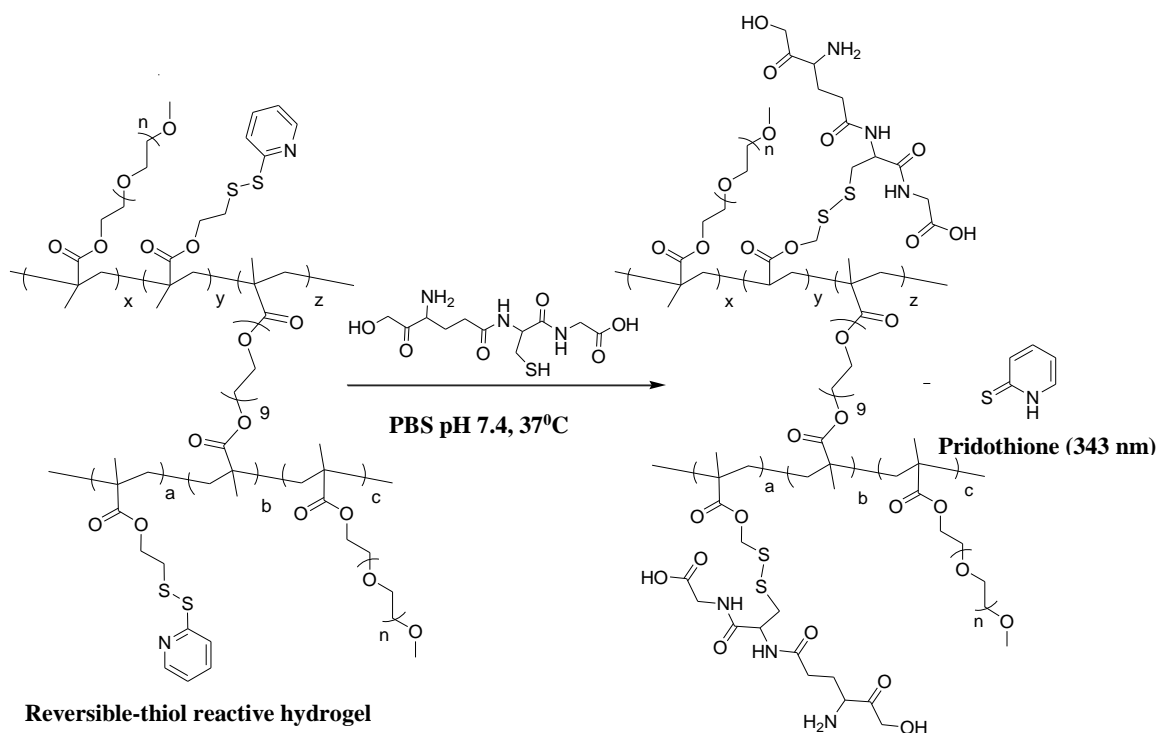


Figure 4.6. Release of pyridothione molecule from the hydrogel by GSH.

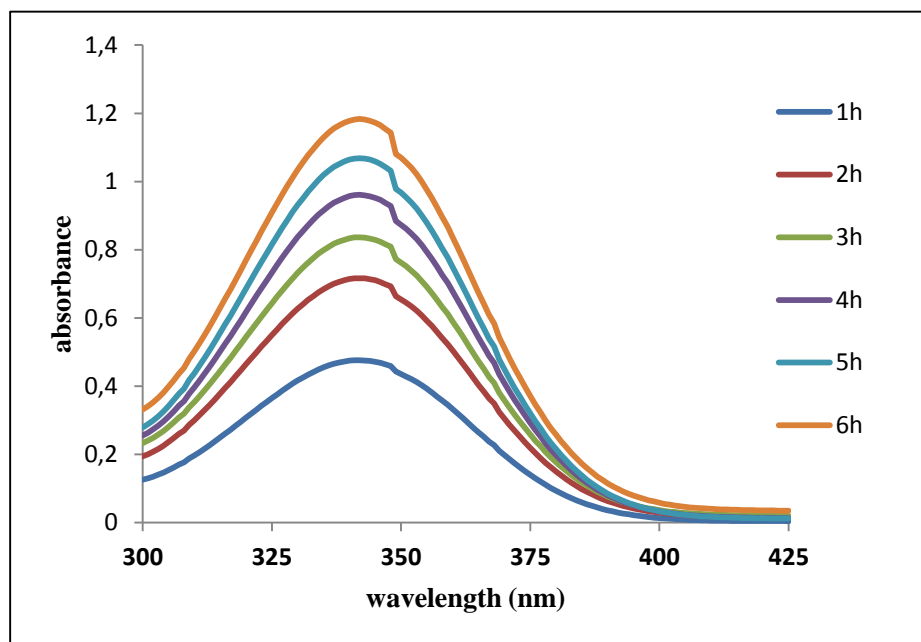


Figure 4.7. Pyridothione release profile of H9 at 343 nm.

Table 4.2. Maximum pyridothione release efficiency (%) of the hydrogels.

Hydrogel/ Time (h)	H4	H5	H6	H7	H8	H9
1	49.7	24.8	2.6	81.1	72.6	29.2
2	68.5	45.2	10.5	88.0	85.5	40.7
3	74.0	56.7	14.2	85.9	87.7	44.3
4	77.0	69.7	21.9	89.0	83.9	47.1
5	80.0	71.8	36.0	99.3	88.6	48.2
6	85.1	80.0	40.4	100	96.5	48.3

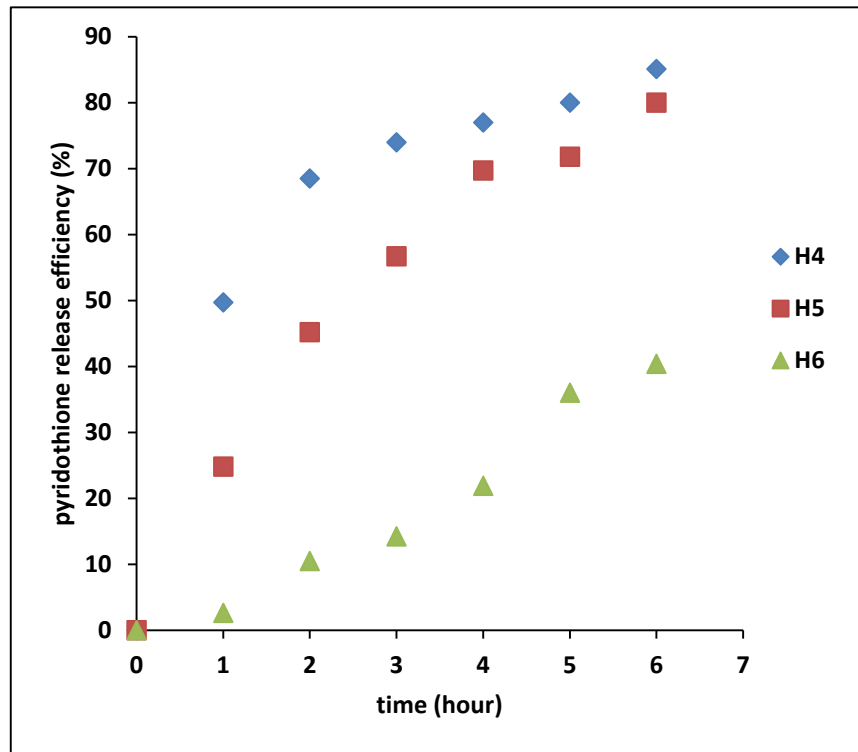


Figure 4.8. Pyridothione release profile of hydrogel H4,H5 and H6.

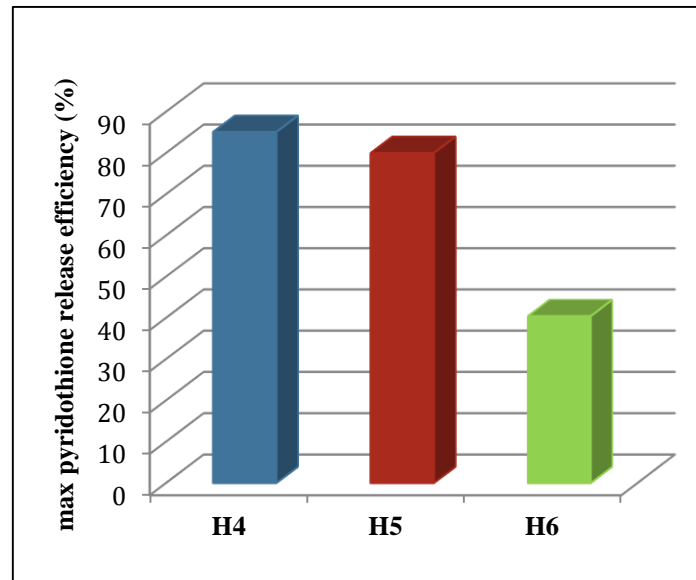


Figure 4.9. Effect of pyridyl disulfide content on pyridothione release.

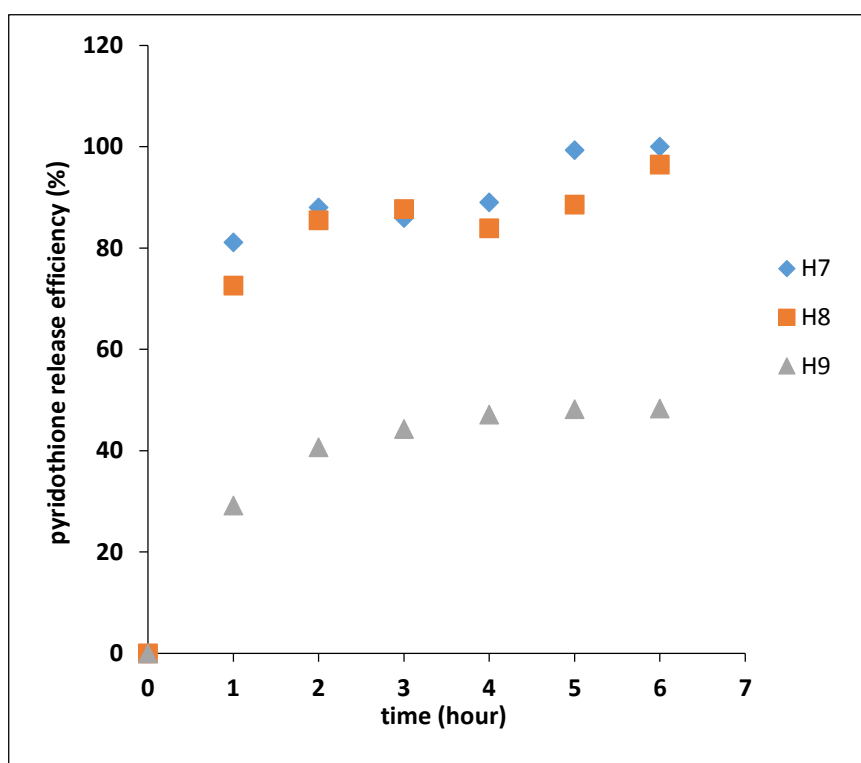


Figure 4.10. Pyridothione release profile of hydrogel H7, H8 and H9.

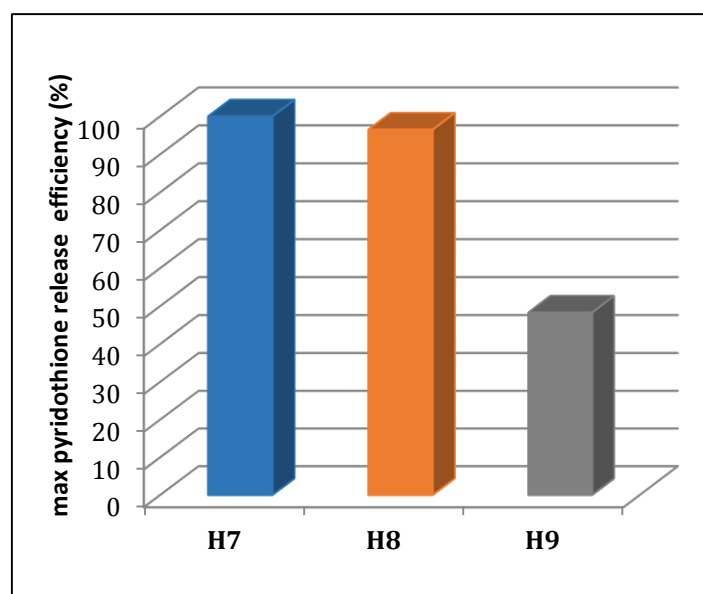


Figure 4.11. Effect of pyridyl disulfide content on pyridothione release.

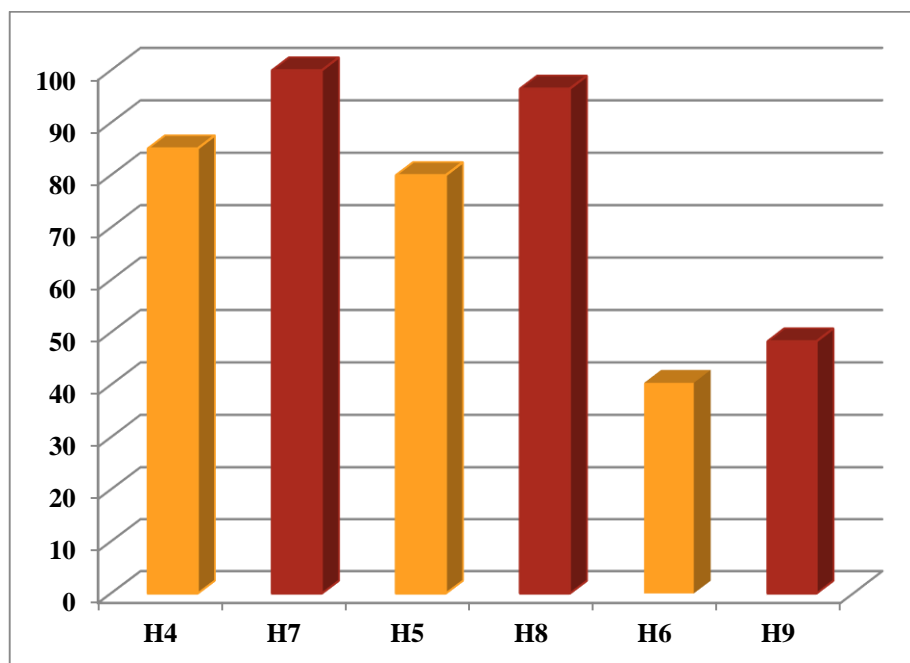


Figure 4.12. Pyridothione release efficiency in H4 and H7, H5 and H8, H6 and H9.

4.2. Reversible-Thiol Reactive Hydrogel Micropatterns

4.2.1. Fabrication of Hydrogel Micropatterns

The fabrication of hydrogel micropatterns is shown in Figure 4.13. Interfacial bonding photopolymerization was used to provide adhesion of hydrogels onto the glass surface. For this purpose, glass surfaces were used and these were treated with 3-Trimethoxysilyl Propyl Methacrylate (TMSPMA). The PDMS stamp was placed on the TMSPMA modified glass wafer and bulk hydrogel precursor mixture was dropped at one of the open ends of PDMS stamp channels and the channel of PDMS was filled with the mixture. After UV exposure, the hydrogel patterns on the glass surface were obtained by capillary reaction with PDMS stamp. The optical microscope images of hydrogel pattern having average width 65 μm were shown in Fig 4.14a and in Fig 4.14b. The results obtained from optical microscope show that three-dimensional hydrogel micropatterns were successfully fabricated via photopolymerization. Since hydrogel patterns have pyridyl disulfide functional groups that are reactive towards thiol groups, they can immobilize thiol containing biomolecules and by using the reversibility characteristic of the patterns, attached biomolecules can be released from the

surface by using thiol groups containing reagents depending on thiol-disulfide exchange mechanism.

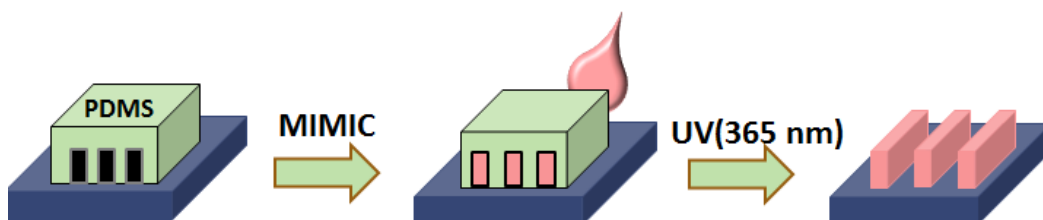


Figure 4.13. Preparation of hydrogel micropatterns.

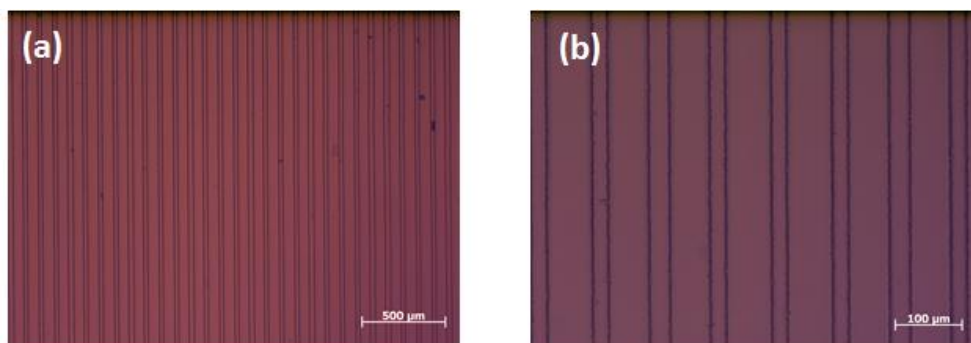


Figure 4.14. Optical microscope images of the hydrogel pattern.

4.2.2. Immobilization and Release of BODIPYC10SH

Reversible-thiol reactive hydrogel micropatterns were functionalized with thiol containing fluorescence dye that is BODIPYC10SH in order to show the capability of the hydrogel patterns to immobilize thiol containing biomolecules. The hydrogel micropatterns were found to be non-fluorescent itself before functionalization as shown in Figure 4.15a. Since the patterns contain pyridyl disulfide functional groups on it, when they were treated with BODIPYC10SH, dye molecules easily bind to the surface by cleaving the disulfide bonds on the hydrogel patterns depending on thiol-disulfide exchange mechanism. Figure 4.15a shows the immobilization of BODIPYC10SH in the hydrogel pattern and results of fluorescence microscope image after BODIPYC10SH immobilization. As expected, after functionalization, nonfluorescent surfaces become

fluorescent indicating the successful attachment of the thiol-containing dye molecules. As a control experiment, hydrogel micropatterns that did not contain any pyridyl disulfide functional group were fabricated by using PEGMEMA monomer and treated with BODIPYC10SH. Fluorescence microscopy results show that there is no covalent attachment of the dye molecules on surfaces (Figure 4.15b). Control experiment proves that the origin of the immobilization of thiol containing molecules is due to the presence of pyridyl disulfide functional groups on the hydrogel microstructures.

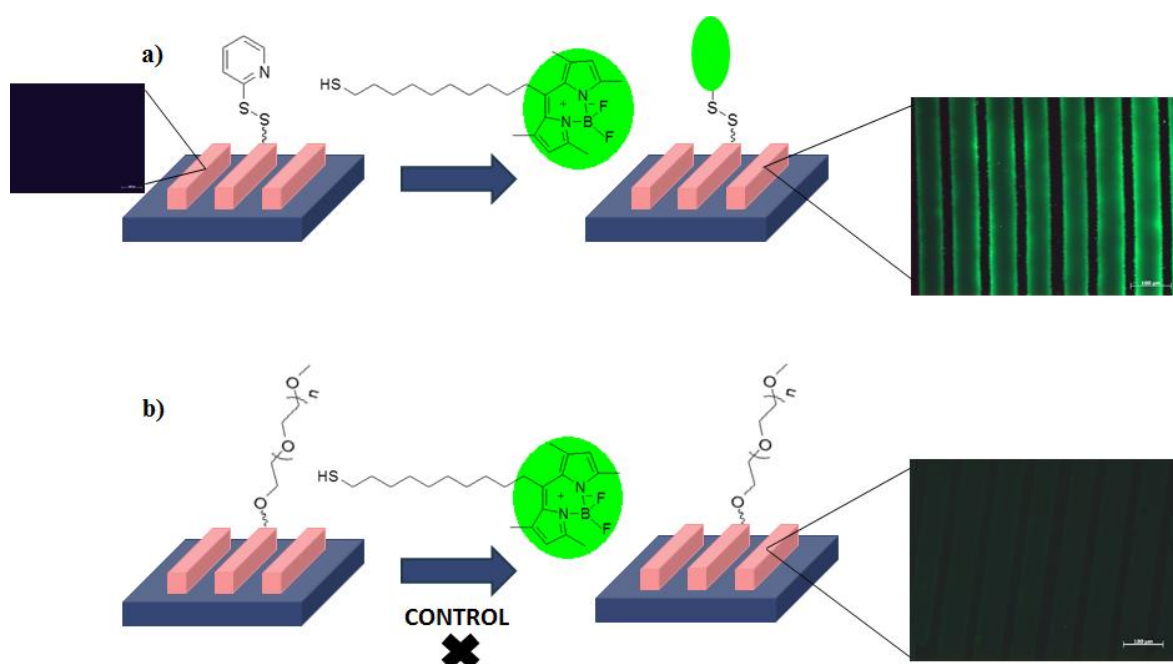


Figure 4.15. a) Functionalization with BODIPYC10SH. b) Control experiment.

After successful immobilization of the BODIPYC10SH on the hydrogel micropatterns, the release of dye molecules from the surface was achieved with thiol containing reducing agent GSH via thiol-disulfide exchange reaction. Thiol groups of GSH cleaved the disulfide bonds and as a result dye molecules were detached from the hydrogel micropatterns (Figure 4.16a). In order to prove that the release of BODIPYC10SH from the micropatterns occurs only in the presence of the thiol containing reagents and not due to hydrolysis, dye immobilized patterns treated with water-THF solution that did not contain any GSH. Fluorescence image results show that there is no loss in fluorescence intensity due to water-THF solvent system and prove that GSH provides the release of

molecules from the patterns (Figure 4.16b). THF was utilized in these experiments as a co-solvent in order to remove the dye molecules, releasing from the hydrogel micropatterns by GSH, since BODIPYC10SH is soluble in THF solvent.

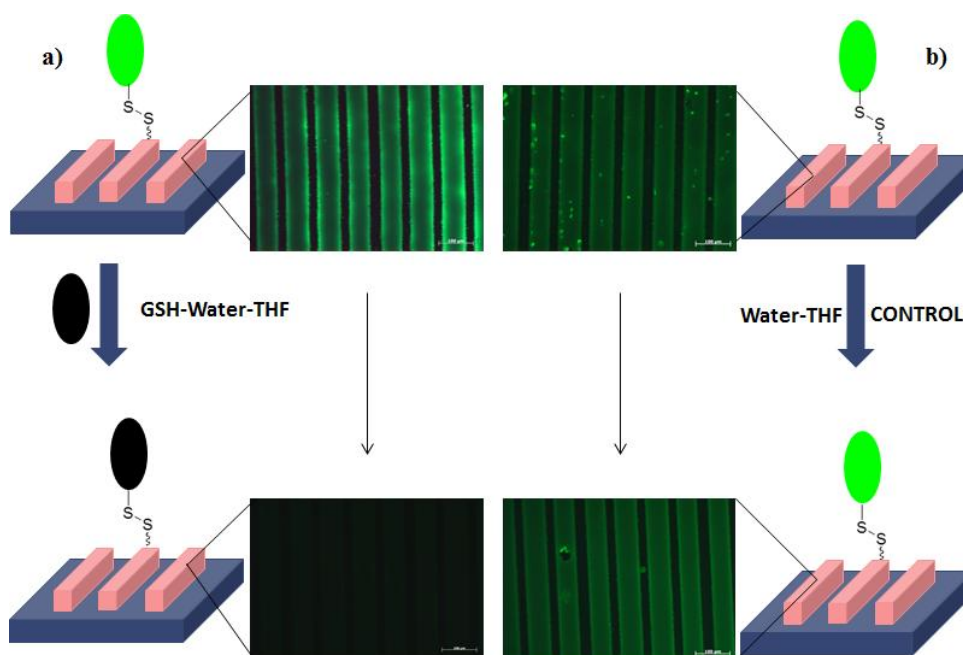


Figure 4.16. a) Release of BODIPYC10SH via GSH. b) Control experiment.

After showing the release of immobilized dye molecules from the patterns by using GSH, another thiol containing reducing agents was used for the same purpose. BODIPYC10SH immobilized patterns were treated with DTT and the release of dye molecules from the surface was achieved depending on thiol-disulfide exchange mechanism. Thiol groups in DTT break the disulfide bonds in the patterns and dye molecules become free and as a result nonfluorescent images confirming the release of BODIPYC10SH were obtained (Figure 4.17). Figure 4.18. shows the relative fluorescence intensities of the hydrogel patterns before and after GSH treatment. After the BODIPYC10SH immobilization on the patterns, fluorescence intensity drops to 91.1 ± 5.8 from 913.0 ± 147.0 with addition of the GSH to the surface. Figure 4.19. shows the relative fluorescence intensities of the hydrogel patterns before and after DTT treatment. After the BODIPYC10SH immobilization on the patterns, fluorescence intensity drops to 69.4 ± 7.1 from 1056.5 ± 79.5 with addition of the DTT to the surface. Since control pattern has no

pyridyl disulfide functional groups, its showing intensity of 77.6 ± 8.3 arises from noncovalent bonding of dye molecules from the surfaces. Since control hydrogel micropattern shows similar intensity with the intensity obtained after DTT treatment, it can be concluded that complete release of dye molecules were achieved with DTT. It is known that DTT is stronger reducing agent than GSH and the experiment results obtained from fluorescence microscope are consistent with this fact. It can be concluded that DTT showed higher efficiency in release of dye molecules from hydrogel patterns comparing to GSH, by providing complete release of BODIPYC10SH.

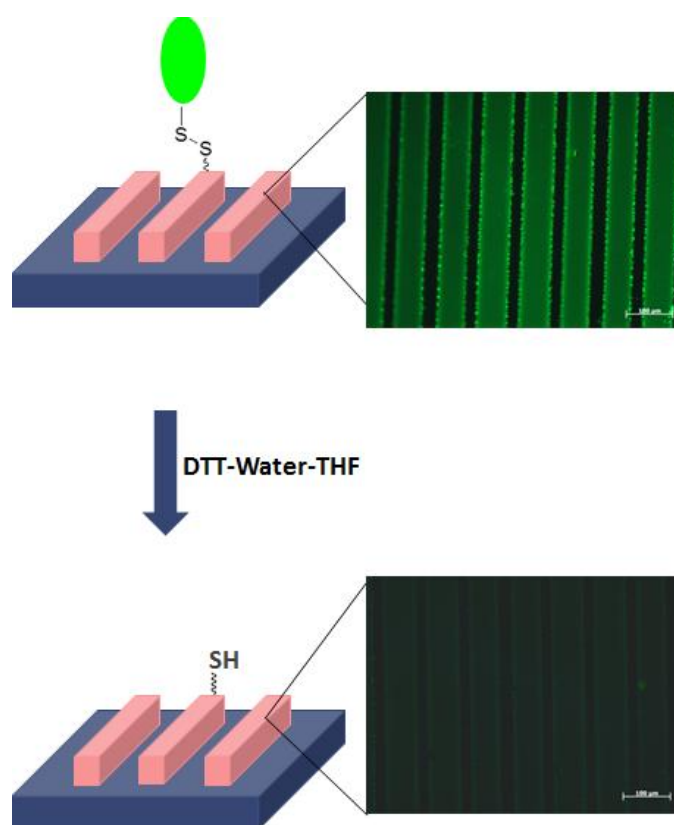


Figure 4.17. Release of BODIPYC10SH via DTT.

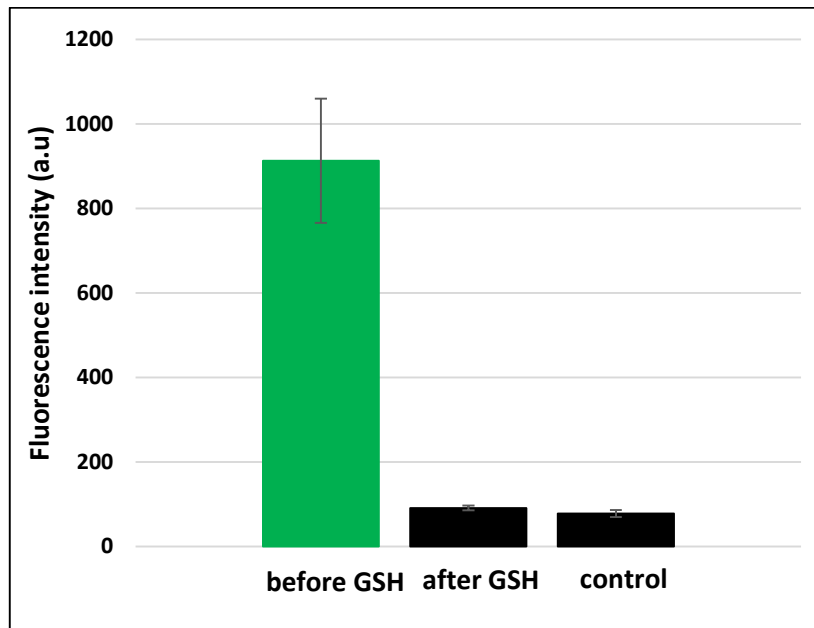


Figure 4.18. Fluorescence intensities before and after GSH treatment, and control.

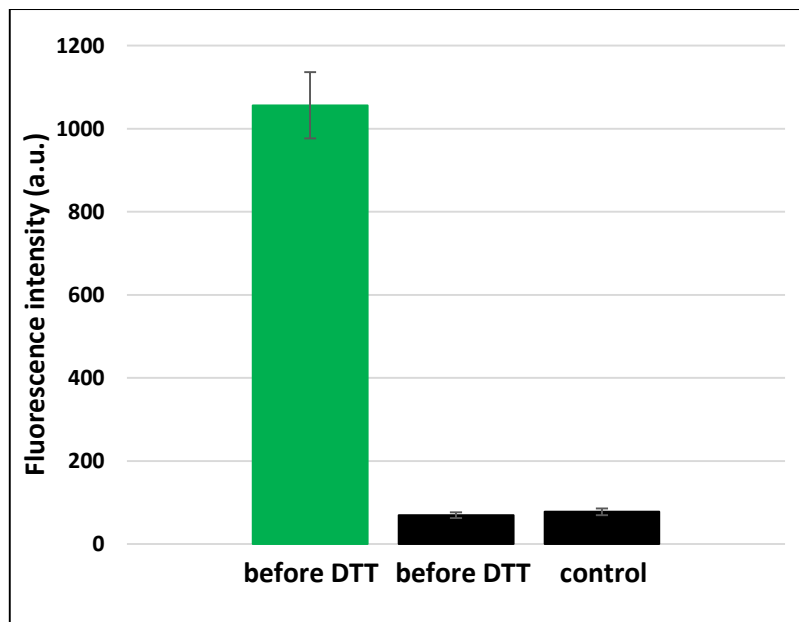


Figure 4.19. Fluorescence intensities before and after DTT treatment, and control.

4.2.3. Immobilization and Release of TRITC-Extravidin

After showing the availability of the fabricated hydrogel micropattern in terms of immobilization and then release of biomolecules with using BODIPYC10SH as a model compound, TRITC-extravidin was immobilized on biotinylated micropatterns and bounded protein was released from the surfaces with DTT as shown Figure 4.20. Micropatterns were conjugated first with thiol containing biotin ligand that is known to bind onto streptavidin through strong specific noncovalent binding. Thiol groups of biotin react with the disulfide bonds in the pattern. The biotinylated surfaces obtained via thiol-disulfide exchange reaction, were exposed to TRITC-extravidin and protein was easily bound to the surfaces and gave red colored image as shown in Figure 4.21b. As a control experiment, a hydrogel micropattern was not biotinylated and results indicate that this micropattern could not immobilize any protein except noncovalently attachment in trace amount and gave dark colored image shown in 4.21a. This experiment proves that the origin of the immobilization of the protein is thiol containing biotin ligand with the thiol disulfide chemistry. As a further study, immobilized protein was released from the surface with the same chemistry in the presence of the thiol containing reducing agent that is DDT (Figure 4.22). DTT cleaves the disulfide bonds and provides the release of bounded protein from the surface. Figure 4.23 shows the relative intensities of the protein immobilized hydrogel micropatterns before and after DTT treatment. It was found that after DTT addition, the intensity dropped to 81.9 ± 6.6 from 902.1 ± 128.6 and also control hydrogel that was not biotinylated shows 78.6 ± 16.7 intensity resulting from noncovalent binding of the protein on the micropattern. Considering the results obtained, it can be concluded that the complete release of covalently bounded protein was achieved in the presence of DTT. Under the light of all conducted experiments it was found that these novel reversible-thiol reactive hydrogel micropatterns are very efficient systems to catch and release of biomolecules.

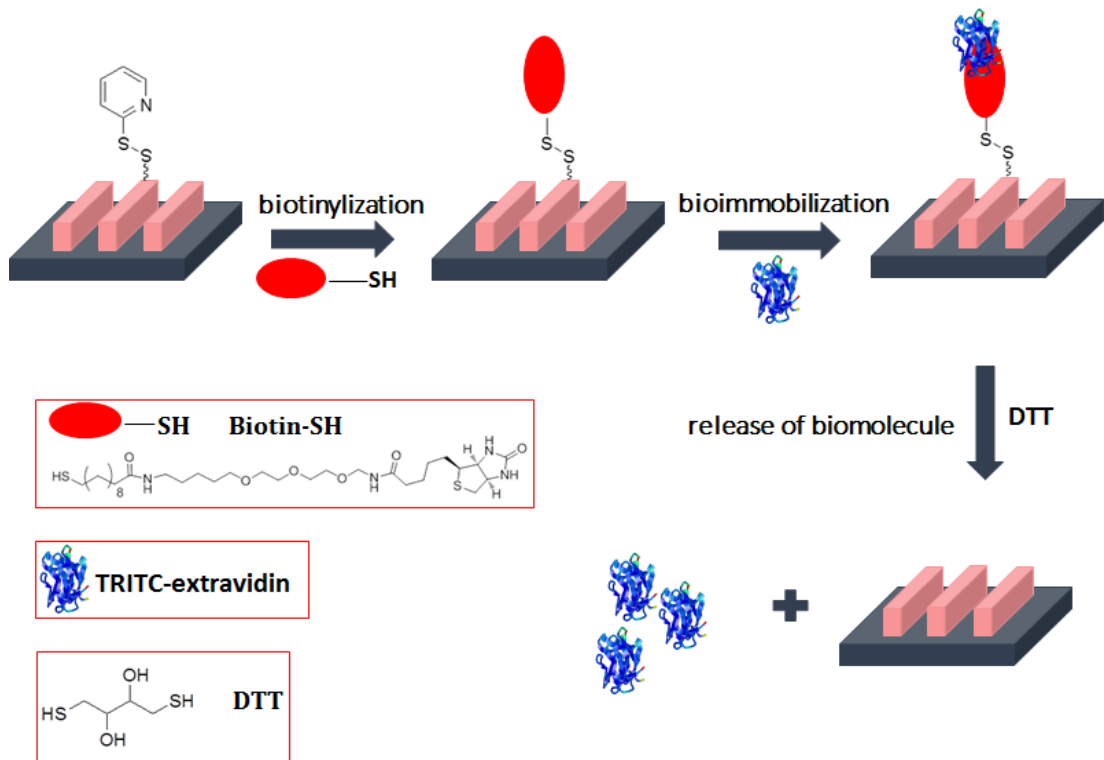


Figure 4.20. Immobilization and release of TRITC-extravidin.

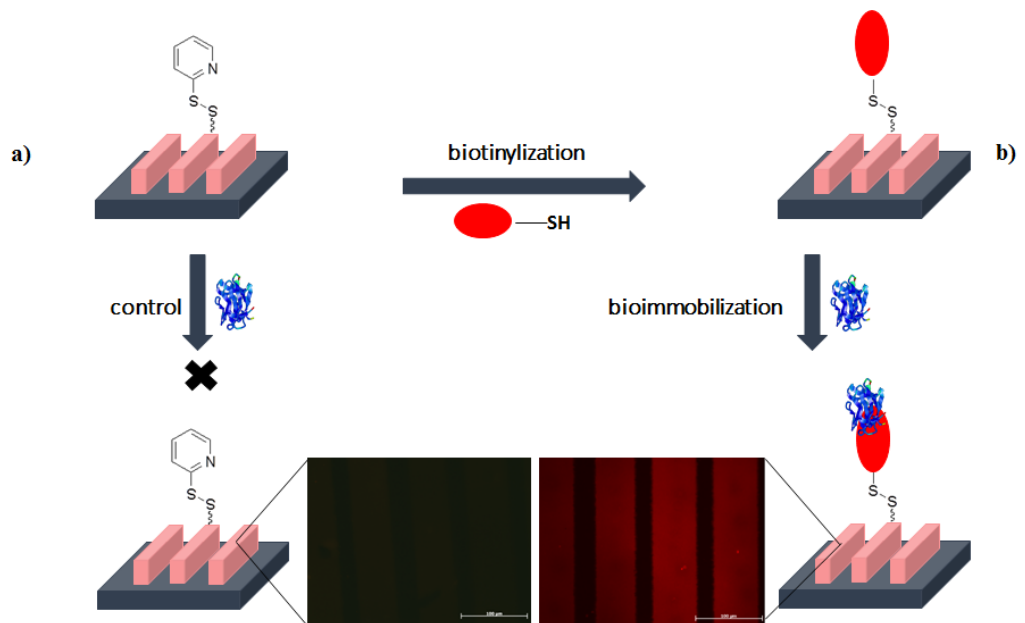


Figure 4.21 a) Control experiment. b) Functionalization with TRITC-extravidin.

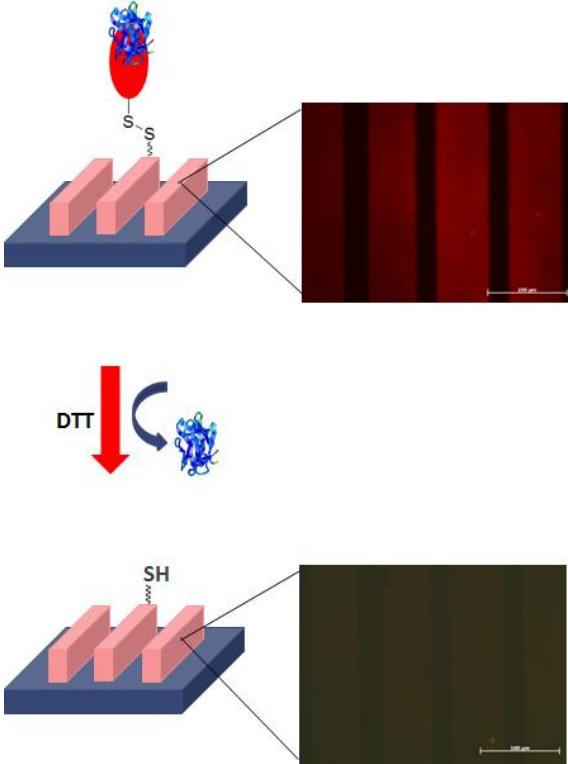


Figure 4.22. Release of TRITC-extravidin via DTT.

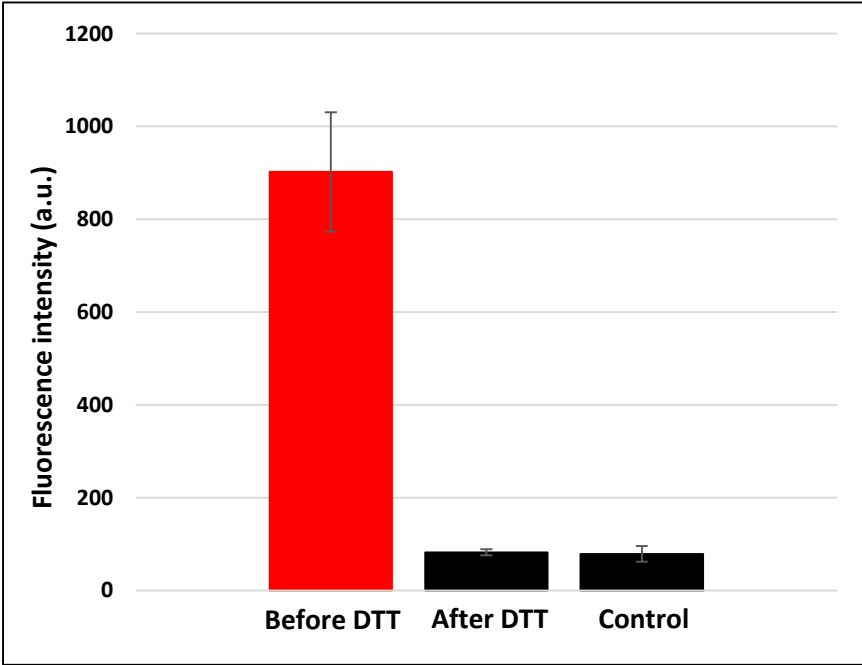


Figure 4.23. Fluorescence intensities before and after DTT treatment and control.

4.3. Orthogonal Thiol Reactive Bulk Hydrogels

4.3.1. Synthesis of Bulk Hydrogels

PEG-based thiol reactive bulk hydrogels containing a certain amount of pyridyl disulfide functional groups and various amount of furan protected maleimide monomer were synthesized by photopolymerization in the presence of DMPA as a photoinitiator and PEGDMA as a crosslinker (Figure 4.24). The orthogonal hydrogel system contains two different functional groups that are pyridyl disulfide and maleimide groups and this property can offer multiple functionalization possibilities. Pyridyl disulfide units can be converted to thiols and protected maleimide groups can be activated by rDA reaction. It is known that maleimide groups are reactive towards thiols but in the hydrogel matrix, two functional groups reactive to each other cannot come together and react with. Also, disulfide linkages are reactive towards thiols and can be used for the reversible incorporation of a biomolecule. Maleimide groups are reactive towards thiol groups and can be functionalized with thiol bearing molecules. By orienting the properties of functional groups, the orthogonal hydrogel system can enable various kind of further functionalities at the same time. The physical and chemical properties of the hydrogels show differences due to changes in the parameters used like ratio between furan protected maleimide monomer and hydrophilic monomer. In order to investigate the role of using various amount of furan protected maleimide monomer, a variety of hydrogels were synthesized. These results are summarized in Table 3.3. and the observations will be discussed after.

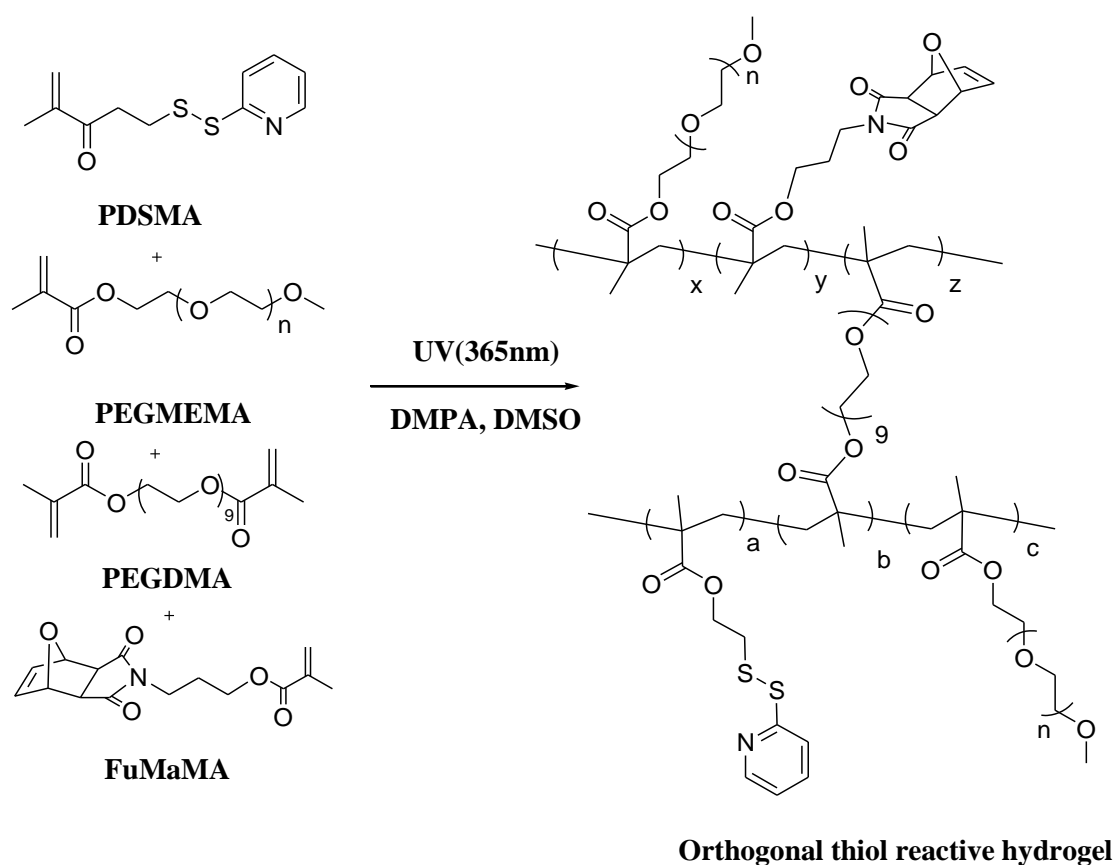


Figure 4.24. Synthesis of orthogonal thiol reactive bulk hydrogels.

Table 4.3. Properties of bulk hydrogels.

Hydrogels	Monomer	Monomer Mw (g/mol)	% Ratio of PDSM:FuMaMA:monomer	Conversion (%)
H1	PEGMEMA	300	10 : 10 : 80	67.0
H2	PEGMEMA	300	10 : 20 : 70	83.9
H3	PEGMEMA	300	10 : 40 : 50	76.7

Photopolymerization condition; PEGDMA = 14.2 mg, DMPA = 5 mg, DMSO = 0.3 mL, UV (365 nm) illumination time = 30 min, room temperature. Conversion (%) = (dry gel weight / total weight of monomer) \times 100.

4.3.2. Thermogravimetric Analysis of Bulk Hydrogels

TGA analysis of the bulk hydrogels were conducted. The TGA results of hydrogels containing FuMaMA show that there is a continuous weight loss starting from 60 to 180°C due the release of furan molecules from the furan protected maleimide groups by rDA reaction [41]. According to the results, it was observed that as FuMaMA percentage within the hydrogel increases, the weight loss consistently increases (Figure 4.25). For example, in hydrogel H3 containing highest amount of FuMaMA led to highest weight loss comparing to hydrogels H1 and H2.

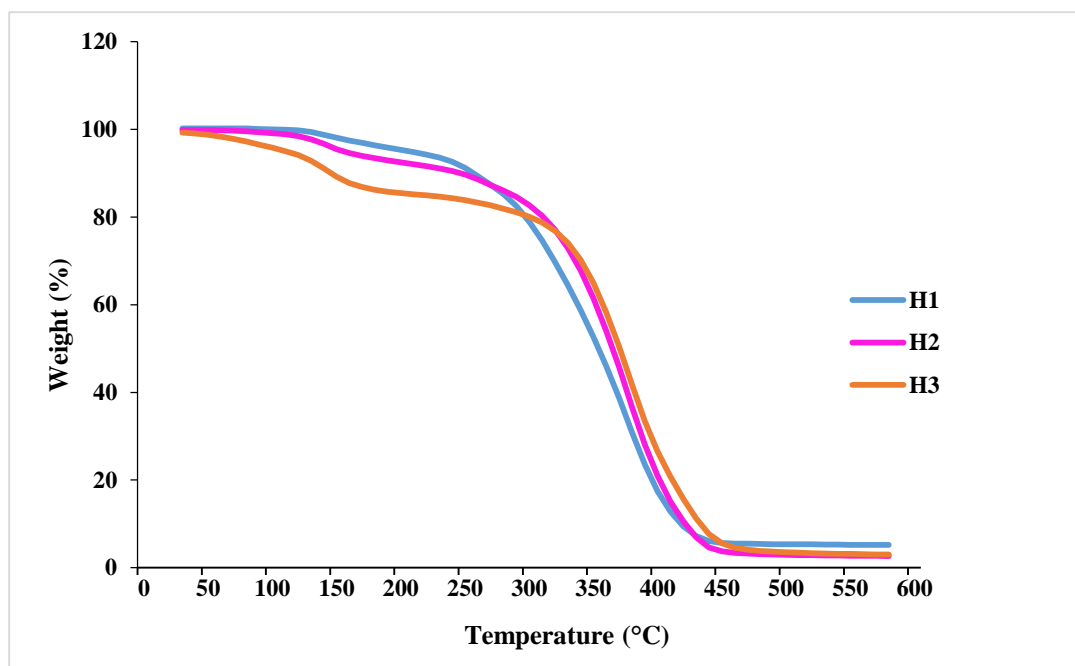


Figure 4.25. Thermogravimetric analysis of the hydrogels.

5. CONCLUSION

In the first part of the study, reversible-thiol reactive PEG-based bulk hydrogels containing various amount pyridyl disulfide functional groups were synthesized by photopolymerization with using photoinitiator and PEGDMA crosslinker. Swelling studies of bulk hydrogels indicate that water uptake capacity of the hydrogels depends on PDSMA content and PEG chain length. In the presence of the thiol containing reducing agent, GSH, pyridothione release profiles of the disulfide functional groups containing bulk hydrogels were obtained via UV-vis spectrophotometer, depending on thiol-disulfide exchange reaction. It was found that the amount of pyridothione release depends on PDSMA content and PEG chain length.

In the second part of the study, reversible-thiol reactive hydrogel micropatterns were fabricated by photopolimerization. These patterns were functionalized first with BODIPYC10SH and the release of fluorescence dye from the reactive pattern surfaces was achieved by using thiol containing reducing agents GSH and DTT separately depending on thiol disulfide exchange chemistry. Further functionalization study was conducted with TRITC-extravidin. Micropatterns were first treated with thiol containing biotin ligand and succesfull attachment of TRITC-extravidin protein on surfaces was shown, also release of the protein was achieved by applying thiol containing reducing agent DTT. Under the light of obtained results, it was found that these reversible-thiol reactive hydrogel patterns are applicable for catch and release of biomolecules.

In the third part of the study, thiol reactive bulk hydrogels containing pyridyl disulfide functional groups and various amount of furan protected maleimide functional groups were synthesized. Thermogravimetric analysis of the hydrogels were conducted and they revealed that a consistent increase in weight loss of the hydrogel was observed upon increasing the amount of FuMaMA.

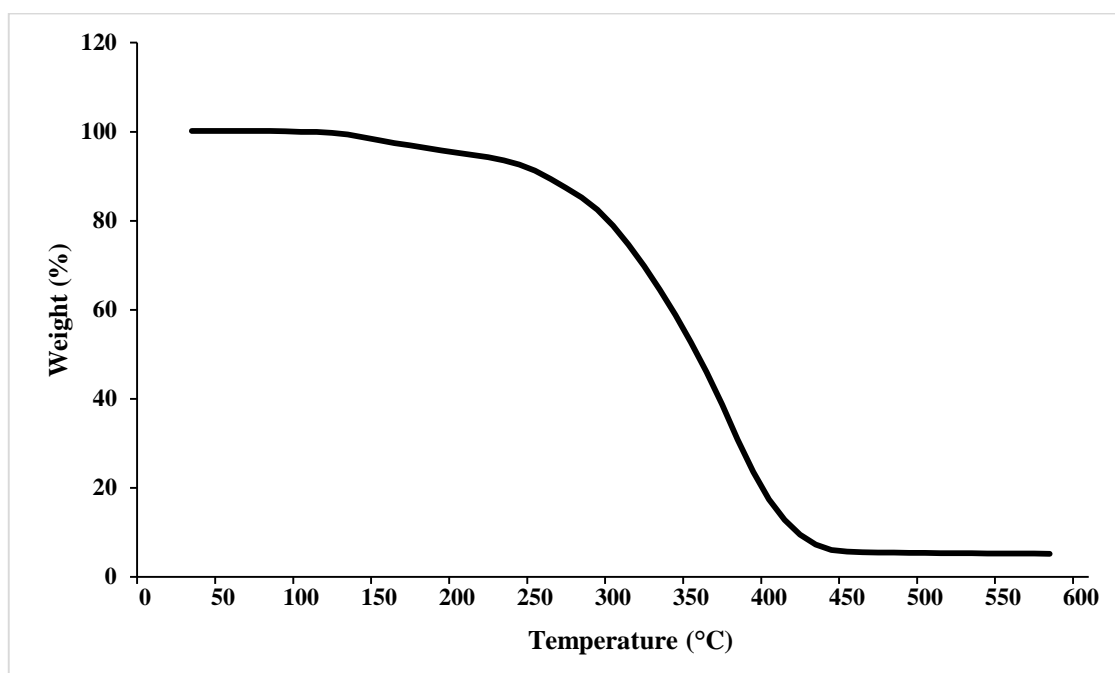
APPENDIX: SPECTROSCOPY DATA

Figure A.1. Thermogravimetric analysis of the H1.

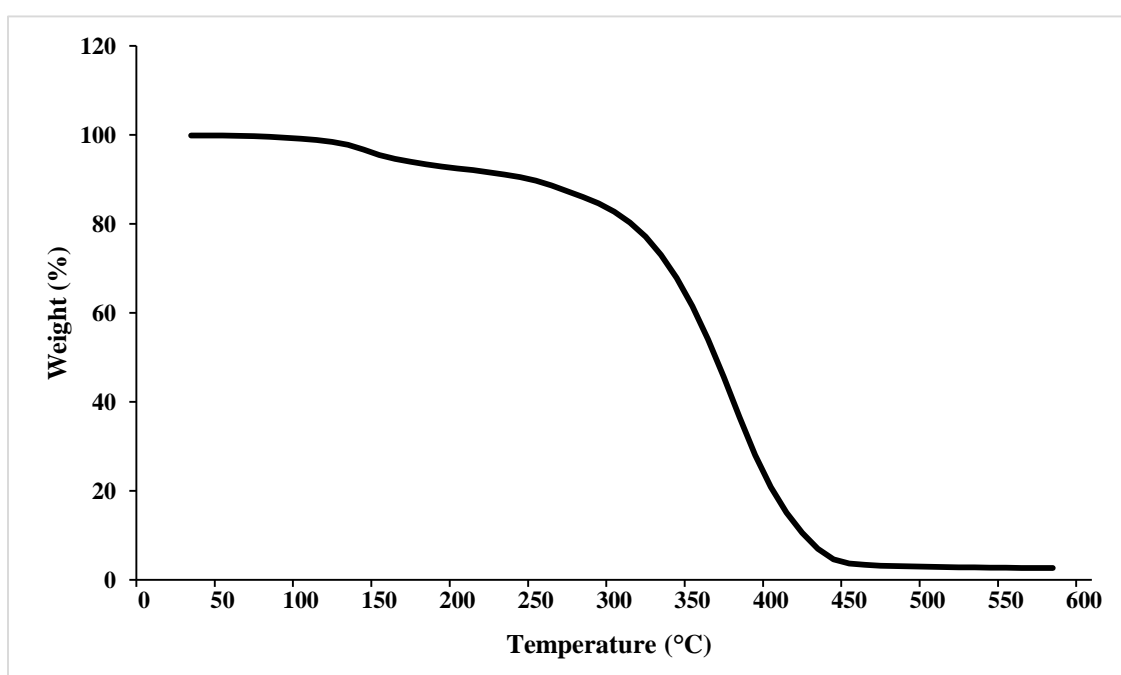


Figure A.2. Thermogravimetric analysis of the H2.

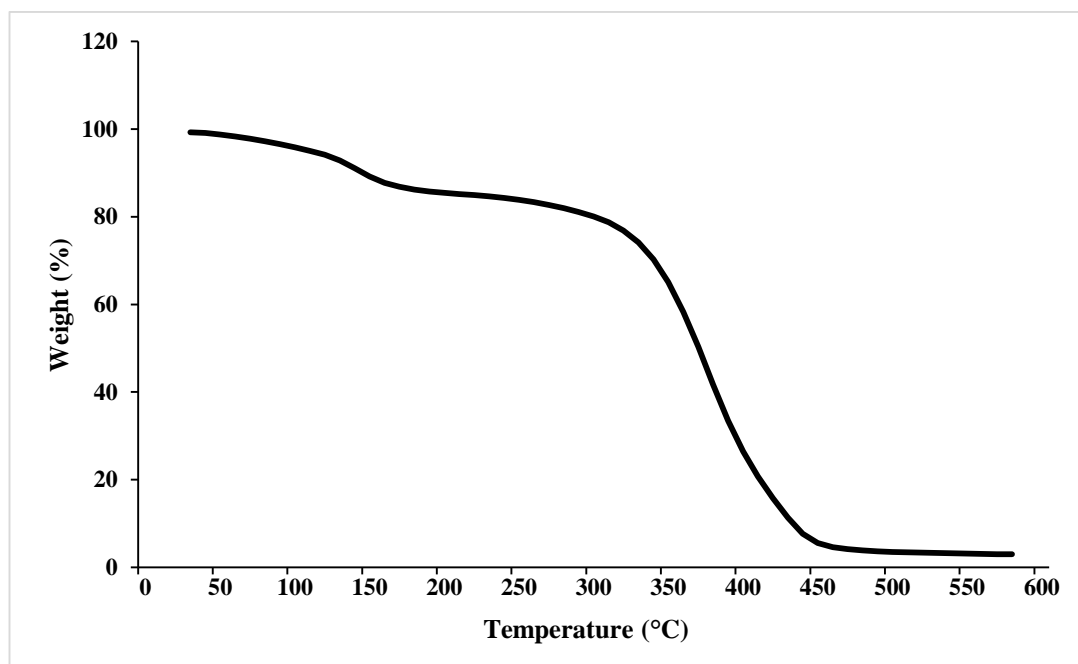


Figure A.3. Thermogravimetric analysis of the H3.

REFERENCES

1. Hahn, M. S., J. S. Miller, and J. L. West, "Three-Dimensional Biochemical and Biomechanical Patterning of Hydrogels for Guiding Cell Behavior", *Advance Materials*, Vol. 18, pp. 2679-2684, 2006.
2. Campoccia, D., P. Doherty, M. Radice, P. Brun, G. Abatangelo, and D. F. Williams, "Semisynthetic resorbable materials from hyaluronan esterification", *Biomaterials*, Vol.19, pp. 2101–2127, 1998.
3. Li, J., "Self-assembled supramolecular hydrogels based on polymer-cyclodextrin inclusion complexes for drug delivery", *Nature Publishing Group Asia Materials*, Vol. 2, No. 3, pp. 112-118, 2010.
4. Vervoort, L. V. G. Mooter, P. Augustijns, and R. Kinget, "Inulin hydrogels. I. Dynamic and equilibrium swelling properties", *International Journal of Pharmaceutics*, Vol. 172, pp. 127- 135, 1998.
5. Lu, Y. and P. S. Low, "Folate mediated delivery of macromolecular anticancer therapeutic agents", *Advanced Drug Delivery Reviews*, Vol. 54, pp. 675-693, 2002.
6. Hongchen, D. and K. Matyjaszewski, "One-Pot Synthesis of Robust Core/Shell Gold Nanoparticles", *Macromolecules*, Vol. 43, pp. 4623-4628, 2010.
7. Wei, H. L., Z. Yang, Y. Chen, H. J. Chu, J. Zhu and Z. C. Li, "Characterization of N-vinyl-2-pyrrolidone-based hydrogels prepared by a Diels-Alder click reaction in water", *European Polymer Journal*, Vol. 46, pp. 1032-1039, 2010.
8. Gupta, N., B. Lin, L. Campos, M. Dimitriou, S. Hikita, N. Treat, M. Tirrell, D. Clegg, E. Kramer and C. Hawker, "A versatile approach to high-throughput microarrays using thiol-ene chemistry", *Nature Chemistry*, Vol. 2, pp. 138-145, 2008.

9. Martens, P. and K. Anseth, "Characterization of hydrogels formed from acrylate modified poly(vinyl alcohol) macromers", *Polymer*, Vol. 41, pp. 7715-7722, 2000.
10. Hoffman, A., "Hydrogels for biomedical applications", *Advanced Drug Delivery Reviews*, Vol. 54, No. 1, pp. 3-12, 2002.
11. Peppas, N. A., "Hydrogels in Medicine", CRS Press Inc., Boca Raton, 1986.
12. Peppas, N. A. and R. Langer, "New challenges in biomaterials", *Science*, Vol. 263, pp. 1715-1720, 1994.
13. Park, K., "Controlled Release: Challenges and Strategies", *American Chemical Society*, 1997.
14. Naota, T. and H. Koori, "Molecules That Assemble by Sound: An Application to the Instant Gelation of Stable Organic Fluids", *Journal of American Chemical Society*, Vol. 127, No. 26, pp. 9324-9325, 2005.
15. Quaglia, F., "Bioinspired tissue engineering: The great promise of protein delivery technologies", *International Journal of Pharmaceutics*, Vol. 364, pp. 281– 297, 2008.
16. Moore, K., M. Macsween and M. Shoichet, "Immobilized concentration gradients of neurotrophic factors guide neurite outgrowth of primary neurons in macroporous scaffolds", *Tissue Engineering*, Vol. 12, pp. 267– 278, 2006.
17. DeLong, S. A., J. J. Moon, J. L. West, "Covalently immobilized gradients of bFGF on hydrogel scaffolds for directed cell migration", *Biomaterials*, Vol. 26, pp. 3227-3234, 2005.
18. Taite, L. J., M. L. Rowland, K. A. Ruffino, B. R. E. Smith, M. B. Lawrence and J. L. West, "Bioactive hydrogel substrates: Probing leukocyte receptor-ligand

- interactions in parallel plate flow chamber studies”, *Annals of Biomedical Engineering*, Vol. 34, pp. 1705–1711, 2006.
19. Chauhan, G. S., S. C. Jaswal and M. Verna, “Post functionalization of carboxymethylated starch and acrylonitrile based networks through amidoximation for use as ion sorbents”, *Carbohydrate Polymers*, Vol. 66, pp. 435-443, 2006.
 20. Witter, A. and H. Tuppy, “N-(4-Dimethylamino)-3,5-Dinitrophenyl)maleimide: A coloured sulfhydryl reagent: Isolation and investigation of cysteine-containing peptides from human and bovine serum albumin”, *Biochimica et Biophysica Acta*, Vol. 45, pp. 429-442, 1960.
 21. Bontempo, D., K. L. Heredia, B. A. Fish, and H. D. Maynard, “Cysteine-Reactive Polymers Synthesized by Atom Transfer Radical Polymerization for Conjugation to Proteins”, *Journal of American Chemical Society*, Vol. 126, pp. 15372–15373, 2004.
 22. Reddick, J. J., J. Cheng and W. R. Roush, “Relative rates of Michael reactions of 2’-(phenethyl)thiol with vinyl sulfones, vinyl sulfonate esters, and vinyl sulfonamides relevant to vinyl sulfonyl cysteine protease inhibitors”, *Organic Letters*, Vol. 5, pp. 1967-1970, 2003.
 23. Kosif, I., E. J. Park, R. Sanyal and A. Sanyal, “Fabrication of Maleimide Containing Thiol Reactive Hydrogels via Diels–Alder/Retro-Diels–Alder Strategy”, *Macromolecules*, Vol. 43, pp. 4140-4148, 2010.
 24. Ghosh, S., S. Basu and S. Thayumanavan, “Simultaneous and Reversible Functionalization of Copolymers for Biological Applications”, *Macromolecules*, Vol. 39, pp. 5595-5597, 2006.
 25. Choh, S. Y., D. Cross and C. Wang, “Facile Synthesis and Characterization of Disulfide-Cross-linked Hyaluronic Acid Hydrogels for Protein Delivery and Cell Encapsulation”, *Biomacromolecules*, Vol. 12, pp. 1126-1136, 2011.

26. Ryu, J., R. T. Chacko, S. Jiwanich, S. Bickerton, R. P. Babu and S. Thayumanavan, "Self-Cross-Linked Polymer Nanogels: Versatile Nanoscopic Drug Delivery Platform", *Journal of American Chemical Society*, Vol. 132, pp. 17227-17235, 2010.
27. Ejaza, M., H. Yub, Y. Yana, D. A. Blake, R. S. Ayyalac, and S. M. Grayson, "Evaluation of redox-responsive disulfide cross-linked poly(hydroxyethyl methacrylate) hydrogels", *Polymer*, Vol. 52, pp. 5262-5270, 2011.
28. Koh, W. G., M. and Pishko, "Photoreaction Injection Molding of Biomaterial Microstructures", *Langmuir*, Vol. 19, pp. 10310-10316, 2003.
29. Lee, S. H., J. J. Moon and J. L. West, "Three-dimensional micropatterning of bioactive hydrogels via two-photon laser scanning photolithography for guided 3D cell migration", *Biomaterials*, Vol. 29, pp. 2962-2968, 2008.
30. Tan, W. A. and T. Desai, "Microfluidic patterning of cells in extracellular matrix biopolymers: effects of channel size, cell type, and matrix composition on pattern integrity", *Biomedical Microdevices*, Vol. 5, pp. 235-244, 2003.
31. Chirra, H. D., D. Biswal and J. Z. Hilt, "Controlled synthesis of responsive hydrogel nanostructures via microcontact printing and ATRP", *Polymers for Advanced Technologies*, Vol. 6, pp. 773-780, 2011.
32. Langer, R. and D. A. Tirrell, "Designing materials for biology and medicine", *Nature*, Vol. 428, pp. 487-492, 2004.
33. Lee, Y., S. Park, S. W. Han, T. G. Lim, and W. G. Koh, "Preparation of photolithographically patterned inverse opal hydrogel microstructures and its application to protein patterning", *Biosensors and Bioelectronics*, Vol.35, pp. 243-250, 2012.

34. West, J. L. and J. A. Hubbell, "Separation of the arterial wall from blood contact using hydrogel barriers reduces intimal thickening after balloon injury in the rat: The roles of medial and luminal factors in arterial healing", *Proceedings of the National Academy of Sciences of the United States of America*, Vol. 93, pp. 13188–13193, 1996.
35. Sawhney, A. S., C. P. Pathak, J. J. Van Rensburg, R. C. Dunn and J. A. Hubbell, "Optimization of photopolymerized bioerodible hydrogel properties for adhesion prevention", *Journal of Biomedical Materials Research*, Vol. 28, pp. 831-838, 1994.
36. Chowdhury, S. M. and J. A. Hubbell, "Adhesion prevention with anicrod released via a tissue-adherent hydrogel", *Journal of Surgical Research*, Vol. 61, pp. 58-64, 1996.
37. Quinn, C. P., C. P. Pathak, A. Heller and J. A. Hubbell, "Photo-crosslinked copolymers of 2-hydroxyethyl methacrylate, poly(ethylene glycol) tetra-acrylate and ethylene dimethacrylate for improving biocompatibility of biosensors", *Biomaterials*, Vol. 16, pp. 389-396, 1995.
38. Pathak, C. P., A. S. Sawhney and J. A. Hubbell, "Rapid photopolymerization of immunoprotective gels in contact with cells and tissue", *Journal of American Chemical Society*, Vol. 114, pp. 8311-8312, 1992.
39. Dispinar, T., R. Sanyal, A. Sanyal, "A Diels-Alder/Retro Diels-Alder Strategy to Synthesize Polymers Bearing Maleimide Side Chains", *Journal of Polymer Science Part A: Polymer Chemistry*, Vol. 45, pp. 4545-4551, 2007.
40. Shepherd, J. L., A. Kell, E. Chung, C. W. Sinclair, M. S. Workentin and D. Bizzotto, "Selective reductive desorption of a SAM-coated gold electrode revealed using fluorescence microscopy", *Journal of American Chemical Society*, Vol. 126, pp. 8329-8335, 2004.

41. Bailey, G. C., T. M. Swager, “Masked Michael Acceptors in Poly(phenylene ethynylene) for Facile Conjugation”, *Macromolecules*, Vol. 39, pp. 2815-2818, 2006.